Chapter

Localization Mechanisms of Radiopharmaceuticals

Sana Komal, Sana Nadeem, Zahra Faheem, Arouma Raza, Komal Sarwer, Hijab Umer, Samina Roohi and Syed Ali Raza Naqvi

Abstract

Scintigraphic techniques have opened a new era of developments in the localization of infectious and cancerous foci. Diseases area targeting mechanisms of radiopharmaceuticals encompasses visualization, characterization, and measurement of physiological and biological functioning at targeted sites in addition to measure the area and density of the disease. The accumulation of a radiopharmaceutical at specific organ is based upon numerous processes such as enzymatic interactions, receptor binding site, transport of chemical species and elimination of damaged cells from circulation by a normal metabolic process. PET and SPECT are developing scanning techniques that provides effective diagnostic tool to identify pathophysiology of diseased cells. In this chapter, we are exploring and explaining different mechanisms of radiopharmaceutical localization for imaging and therapeutic processes. The knowledge of these mechanisms will help to develop target based new radiopharmaceuticals using variety of medically used radioisotopes either for imaging or therapy of diseased cells.

Keywords: radiopharmaceuticals, SPECT imaging, antibiotics, infections, cancer

1. Introduction

Dysfunction and disruption of healthy physiological and biochemical cycles lead to the formation of malignancies. As the treatment of many diseases involves biochemical reactions so it may provide a basis for diagnosis. Several radiopharmaceuticals widely available that use to visualize the functioning and structure of body cells, tissues, and organs. These radiopharmaceuticals formulated for treating several malignancies, pain palliation due to bony metastases, joint diseases, and many other similar conditions. Nuclear medicine basically, a medical specialty comprises a carrier molecule and radiotracer that image the regional biochemistry of the body. The biochemical nature of carrier molecule and radiotracer; effects on organ uptake, retention, transportation and biodistribution towards targeted area. So, it's essential to know about the biochemistry of radiopharmaceuticals for better understanding [1]. Nuclear pharmacists must understand how radiopharmaceuticals localize and initiate its work, aka action mechanism. This expertise was required to assess the substrate specific and non-specific nature of labeled drug, its pharmacokinetics and biodistribution because life matters. As the radiopharmaceuticals provide us an opportunity for timely diagnostics using blood flow,

multi-molecular cell localization, bio-energies, tissue metabolism, physiological functioning of the organ, intercellular and intracellular communicative pathways [2]. Different radiopharmaceuticals are used to image different organs based on the functioning of the organ. For example, the labeled iodine would be ideal for imaging thyroid malignancies, because inorganic iodine absorbed more in the thyroid. Similarly, radiolabeled phosphate widely used for the bone scan as it is observed that phosphate ions more accumulated in the bone. Hence one can use the same labeled atoms for organ imaging, which are more accumulated there.

A radiopharmaceuticals localization mechanism is specific to targeted organs depends on processes as varied as antigen–antibody reactions, physical particle trapping, receptor site binding, removal of deliberately damaged cells from circulation, and transportation of a chemical species across a cell membrane and into the cell via a normally operational metabolic cycle. Chemically, radiochemistry plays a crucial role in producing these compounds and in conducting quality assurance procedures to ensure purity [1, 3].

Some other factors also important for the selection and action of radiopharmaceuticals like for diagnosis gamma emitters were preferably choose (beta emitter in case of therapeutic), energy threshold 100–250 Kev, high T/NT ratio last but not least t_{eff} must be moderately long.

Furthermore, insoluble radiopharmaceuticals such as ^{99m}Tc-MAA and ^{99m}Tc-SC are used to represent the lungs and liver/spleen, diagnostic tests, respectively. Since it is well known that these two organs extract particles from the bloodstream, selection based entirely on particle size instead to chemical composition.

The mechanisms explained are not specific to radiopharmaceuticals, but these may be appropriate for some instances to explain the localization mechanisms of nuclear medicines. Radiopharmaceuticals are not limited to a mechanism but requires a combination of more than one mechanism. Lastly, a comprehensive overview of radiopharmaceuticals characteristics, their mode of action and detailed examples are given.

2. Mechanism of localization

The success of the molecular imaging technique using radioisotope labeled molecules commonly termed as radiopharmaceuticals relies on the mechanism of localization at disease cells. In the following sections we are explaining different mechanisms of radiopharmaceutical localization undertaken either for imaging process or therapy of diseases.

2.1 Compartmental localization

Generally, the phenomenon in which the desired species are disseminated in a bounded space is named as compartmentalization or may also be termed as compartmental localization and basically this bounded space is called as a compartment. Specifically, in radio pharmacy compartment-localization means to put a radiotracer in a bounded space and sustaining the tracer for time being enough to scan that bounded space. The bounded space contains fluids (either liquid or gas). The fluids of compartment move systematically in normal circumstances but the pathophysiological changes cause anomalies in the motion of compartmental fluids. These conditions if left unattended and untreated may become fatal. But the conventional diagnostic techniques fail to localize the exact location of abnormality, so, here radio pharmacy provides refuge and we can get exact pinpoint location along with treatment from molecular imaging.

The compartments in biological systems are: Vascular system (blood vessels), Airways of lungs, cerebrospinal fluid (CSF) space, Abdominal (peritoneal) cavity, Alimentary (digestive/GI) tract, urinary system, lymphatic vessels.

The compartmental localization could be in the form of:

a. Uniform distribution inside compartment

b. Non-uniform distribution within compartment

c. Outflow from compartment

d. Flow within the compartment

2.1.1 Uniform distribution inside compartment

Vascular system is the most typical example of uniform dispersion inside compartment. By utilizing the tracer dilution method blood volume could be analyzed quantitatively. A radiopharmaceutical named I-125 RISA (Radio-Iodinated Serum Albumin) diffuses uniformly in blood plasma, is employed to determine volume of plasma in blood.

- Cr-51 labeled RBCs is another radiotracer that is applied to evaluate the mass of red cells (volume of red cells in blood). This radiotracer distributes itself inside the blood's cellular part uniformly.

- Another radiotracer technetium-99 m labeled RBCs homogenously diffuses in blood, is used to evaluate expulsion fraction of left ventricle and movement of left ventricular wall by using gated blood-pool scanning.

2.1.2 Non-uniform distribution within compartment

Radiopharmaceuticals are not distributed equally every time. In some conditions they exhibit non-uniform dispersion, therefore showing disordered physiological process (due to some disease or injury). The increased concentration of a radiopharmaceutical in any organ or tissue corresponds to the disturbance in normal physiological function of that organ or tissue (pathologic changes).

Examples:

- Hemangioma is a condition in which a bright-red bump having extra blood vessels appears on skin and is quite rubbery. Extra blood vessels mean extra blood in that region. So, technetium-99 m labeled RBCs shows amplified localization in this region due to escalated volume of blood.

- Hydronephrosis is the inflammation of a kidney triggered by the accumulation of urine in kidney. This condition prevails when urine could not be drained out from kidney to bladder owing to some sort of obstruction or blockade. MAG3 and DTPA radiolabeled with ^{99m}Tc are used for its imaging. But, MAG3 has preference over DTPA due to its good output. Mercaptoacetyltriglycine (MAG3) is a peptide radiolabeled with ^{99m}Tc and it is released in kidney tubules. So, this increased volume of urine results in escalated amount of ^{99m}Tc-mertiatide (MAG3) or ^{99m}Tc-pentetate (DTPA) tracer in affected kidney.

The decreased concentration of the radiotracer in a compartmental cavity is usually the outcome of block in the cavity as mentioned in following examples:

- Xenon-133 ventilation imaging of lungs is used to confirm the obstruction in airways of lungs. This radiotracer will not be present past the block in the case of complete obstruction. While in partial hindrance, Xenon-133 would not be present in affected region after preliminary breathing but with time thru equilibrium rebreathing the radiotracer travel through the areas of partial hindrance.

- The obstruction in cerebrospinal fluid space could be monitored by intrathecal injecting ^{111}Indium-pentetate (DTPA). After injection ^{111}Indium-DTPA normally drifts up the spine and all over the brain. But in case of obstructing hydrocephalus, hindrance impedes the movement of ^{111}In-DTPA [4].

2.1.3 Outflow from the compartment

An uncharacteristic escape of content from compartmental space occurs owing to some pathologic changes (disturbances in normal physiological function). Radio pharmacy has a good lot of tracers that can precisely sense and find the location of compartmental leakage.

2.1.3.1 Mechanism of technetium-99 m labeled RBCs

Technetium-99 m labeled RBCs are used to foresee the exact location of Gastrointestinal bleeding. Because the blood from hemorrhaged vessel leaks-out and piles in GI-tract. So, radio-images using technetium-99 m labeled RBCs tracer shows the exact pinpoint location of hemorrhage.

After administration, technetium-99 m labeled RBCs speedily disperse in the vascular spaces. Small amount to activity could be observed in the urinary tract, that is due to free activity. No considerable GI bleeding is visualized in the early angiographs. But with time lapse the angiographs shows the bleeding in case of hemorrhage (blood move out of the disrupted area and the tracers in blood give exact scan of image [5].

The other examples include:

- ^{111}In-DTPA imaging is employed to demonstrate the leakage of cerebrospinal fluid.

- Post cholecystectomy, ^{99m}Tc-disofenin or ^{99m}Tc-mebrofenin could be used to monitor whether the bile is leaking out in abdomen or not.

- The ^{99m}Tc-MAG3, a peptide, binds ^{99m}Tc and could be employed to assess reno-vascular hypertension, kidney-transplant, hydronephrosis and urological anomalies. ^{99m}Tc-MAG3 (mercaptoacetyltriglycine) is also used to track leakage of urine into the abdominal cavity. Usually after kidney or urinary tract surgeries this complication occurs and urine seeps into the abdominal cavity.

2.1.4 Flow within the compartment

The changes in extent, rate and direction of compartmental flow is the consequence of some pathophysiological changes, that needs to be assessed and treated.

^{99m}Tc-sulfur colloids is preferably used for studying the rate at which gastric contents are emptied in the stomach by. The reason why ^{99m}Tc-sulfur colloid is suited for this study is that it is not absorbed by Gastrointestinal tract. For assessment of solid emptying rate ^{99m}Tc-sulfur colloid is bound in scrambled eggs, while for liquid emptying rate ^{99m}Tc-sulfur colloid is mixed in drinking water. Then experimental values are compared to normal values with a margin of ±2 standard deviation. The presence and rate of back reflux of contents (due to infections) of urinary bladder to kidney is also studied by the scans taken at specific time lapse using ^{99m}Tc-sulfur colloid (SC). This tracer is implanted by means of a catheter in bladder [6].

2.2 Passive diffusion/simple diffusion

Passive diffusion refers to the random motion from higher to lower concentration of molecules to attain uniformity. Diffusion of tea into water from teabag is most common example of passive diffusion. But typically, in a biologic system this movement comprises motion of molecules across the membrane. Factors like pH, ionization, size of molecule and lipid solubility affect the mobility of molecules to move across the membranes.

Lipid solubility is the primary factor as phospholipids, glycolipids, sphingolipids, and sterols are the common types of lipids that make up membranes, of which phospholipid is the chief constituent. So, only the molecules that are soluble in lipids (lipophilic) could move across the membranes while polar hydrophilic molecules could not cross the membrane system.

pH and ionization impact also influence the mobility of molecules, as all molecules bear different charge (either neutral or charged according to pH). As pH varies the ionization state also varies. Like amines maybe neutral at high pH values and protonates at low pH values. So, according to the pH of surrounding, molecule could not move across membrane when ionized state (hydrophilic), but same molecule could pass when in non-ionizes state (lipophilic).

Size of molecules is another important parameter, allowing only molecules of certain size to pass through the pores on membranous surface. Generally, the particles that weigh less than 80 Daltons could pass only, the entry of molecules greater than this size is thus restricted.

There are certain characteristics of passive diffusion:

- Concentration gradient is required for this type of movement. The membranes in human body segregates this concentration gradient so, in biologic systems it is movement across the membrane (from higher to lower concentration).

- It is fast at high conc. Gradient and slow at low conc. Gradient.

- It does not need any sort of input as it is a passive method.

- It is a non-selective process because no carriers or receptors are included in this method.

Many radiotracers are localized in the targeted organs by mechanism of passive diffusion. And its flow is invariably from areas of high tracer concentration to lower. Initially, diffusion rate is in direct proportionality to the tracer concentration, until equilibrium is achieved. ^{133}Xe,^{127}Xe, and ^{81m}Kr are commonly used for ventilation and have non-reactive lipophilic nature. After administering the tracer via inhalation, diffusion process operates, and the ventilation gas is scattered in airways

of lungs. The flow is smooth until and unless discontinued due to the presence of hinderance in airways. After entering the pulmonary circulation, gases leave lungs by alveolar-capillary diffusion method.

2.2.1 Mechanism of ^{99m}Tc-DTPA (diethylene triamine penta-acetic acid)

A chief factor that has a key role in localization mechanism of radio tracer in brain region is barrier of blood and brain (brain–blood barrier/BBB). It is basically a uniform film of endothelial cells belonging to cerebral vessels, restricting the diffusion of lipophobic molecules, and allowing only lipophilic ones. Due to some physiological abnormalities, this barrier is interrupted allowing the diffusion of hydrophilic molecules in tissues of brain. Oxygen, electrolytes, CO, glucose, water and other smaller molecules diffuses passively in across barrier and use active mechanism to move in the neural cells, while immuno-globulins (large particles), many lipophobic radiotracers and other lipophobic (hydrophilic) particles cannot cross the barrier under normal circumstances but in situations when barrier is disrupted the radiotracers accumulate at the area of tumor/abnormality easily, showing a + scan.

A typical radiopharmaceutical for brain imaging by ^{99m}Tc-DTPA. Normally, it cannot diffuse across barrier easily because of its lipophobic nature (See **Figure 1(A)**), but in abnormalities like tumor and infections the barrier is disturbed, so, ^{99m}Tc-DTPA move passively across barrier and amass in the infected area of brain (See **Figure 1(B)**). Its biologic half-life is 1–2 hours, halftime for clearance of plasma is 70 minutes and in 24 hours 90% of the tracer is eliminated by urinary system.

10–20 millicurie of ^{99m}Tc-DTPA is injected intra-venously in the body and after an hour scanned via gamma cameras. If the scan shows no agglomeration of radiotracer in brain, it means that the barrier is intact, and the tracer was not able to past across the barrier. But if the scans show tracer concentration in the cells of brain it means the barrier is no more intact and is prevailed by anomalies. So, the tracer highlights the affected areas as hot-spots [7].

Other examples:

Other radiotracers that are involved in such type of study (that localize passively in brain) are ^{99m}Tc-glucoheptonate (GH), ^{123}I-serum albumin, technetium pertechnetate ($^{99m}TcO_4^-$) [9], Thallous chloride Tl-201 [10, 11], Gallium citrate Ga-67 [12].

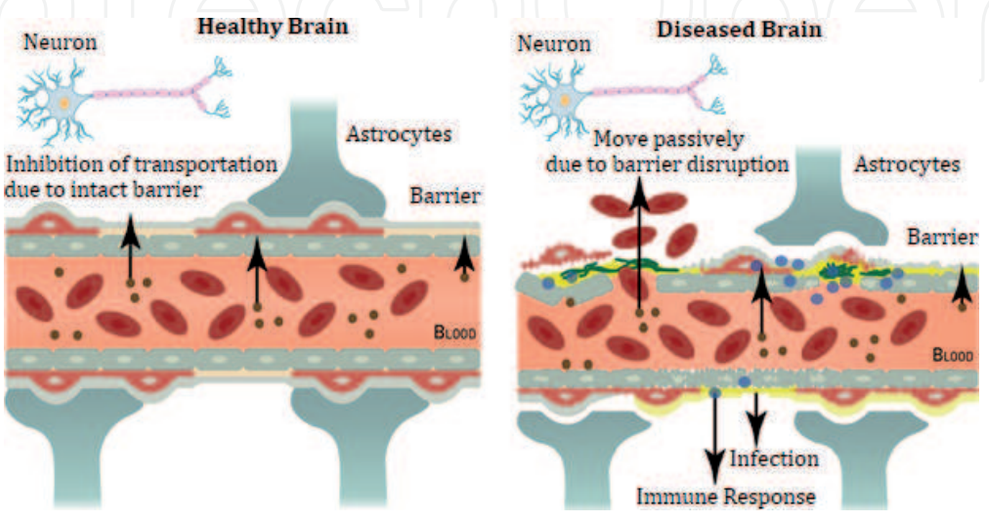

Figure 1.
(A) Illustration of intact barrier in the brain cells that do not allow ^{99m}Tc-DTPA to diffuse, (B) disruption of barrier in the brain cells [8].

2.2.2 Mechanism of ^{99m}Tc- Sestamibi

^{99m}Tc labeled cationic, lipophilic tracers like furifosmin, tetrofosmin and Sestamibi for myocardial perfusion imaging have been established. ^{99m}Tc-Sestamibi is some-what similar to cationic $^{201}Tl^{+}$ but Sestamibi transport across the membrane only involves passive diffusion [13]. In start, it was assumed that the uptake of technetium labeled Sestamibi by the myocardial cells is primarily because of binding of lipid constituents to the membrane of cell. This ambiguity was later cleared that uptake was not because of membrane's binding to lipid constituent, instead the cellular entry is chiefly linked to mitochondria and its negative potential of inner membrane. About 90% of uptake was linked to mitochondria [14] (See **Figure 2(A)**). It was studied that the upholding of technetium labeled Sestamibi is not specific to tumor of some organs, rather it is a general mechanism.

^{99m}Tc- Sestamibi moves passively from blood to tumor and amass in the cancers that have low multidrug-resistant pump expression and more mitochondria making cancers susceptible to precise diagnosis. But in most cases, the resistance pump dominates over mitochondrial presence making cancers non-susceptible to ^{99m}Tc-Sestamibi, because the resistance pumps eject the radiotracer out of the cell [15]. So, the upholding status of this radiotracer reflects the membrane permeability of mitochondria and the mitochondrial potentials. Alterations due to cancers leads to dys-functioning of mitochondria that consequently cause decreased uptake of tracer [16] (See **Figure 2(B)**). The decreased upholding of technetium Sestamibi in the terms of chemotherapy (after chemotherapeutic session) is correlated to the over-expression of multidrug-resistant proteins. So, the cancers which do not uphold this tracer are not prone to chemotherapy.

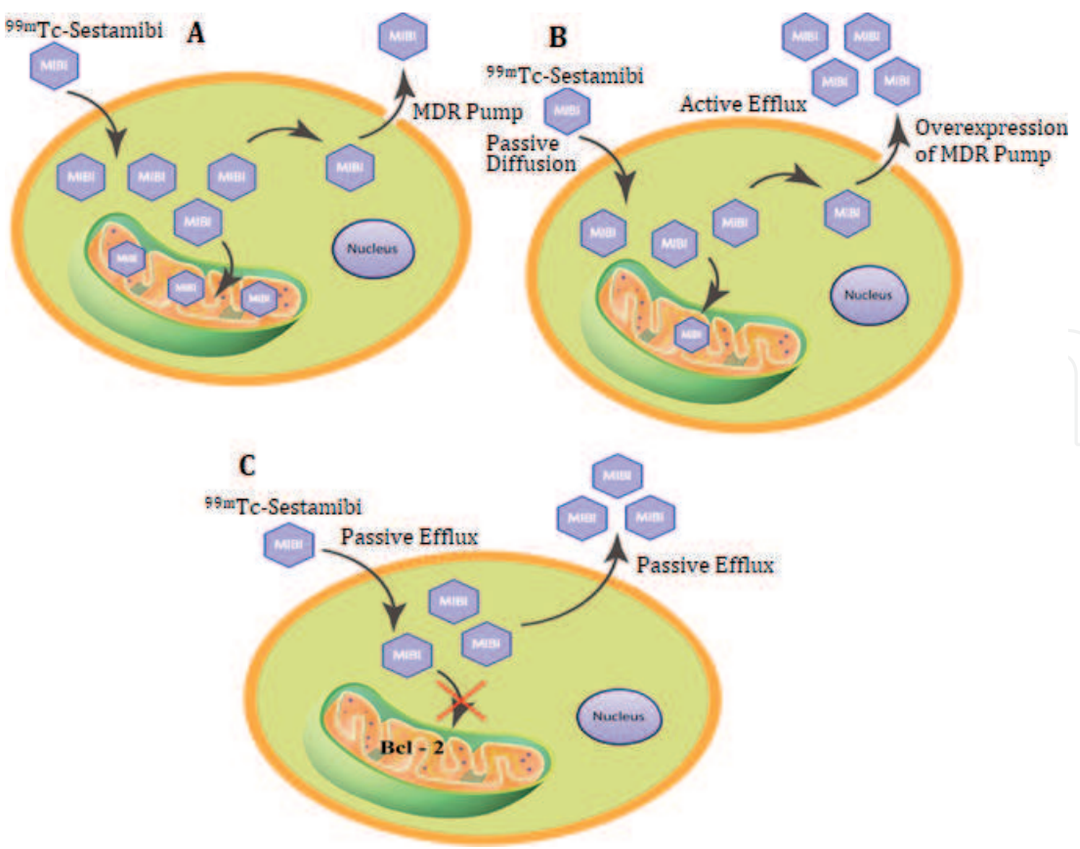

Figure 2.
(A) Normal binding of ^{99m}Tc- Sestamibi to mitochondria, (B) over-expression of resistance pump that quickly removes ^{99m}Tc-sestamibi out of cell, (C) effect of Bcl-2, an anti-apoptotic protein; that halts the binding of ^{99m}Tc-sestamibi to mitochondria [17].

The other possibility is that the protein that prevents the induction of apoptosis (Bcl-2, prevents the membrane permeability of mitochondria) maybe over expressed, halting the entry of radiotracers in mitochondria [18] (See **Figure 2(C)**).

Few compounds to suppress/neutralize the effects of anti-apoptotic protein have been subjected to clinical trials. The purpose for this is to monitor the credibility and efficacy of ongoing therapeutic procedure.

2.3 Phagocytosis

The word "Phagocytosis" derived from Greek language that translate as "CELL EATING" (a procedure in which cell engulfs a particle and internalizes it). A prime example involves Kupffer cells (that present in the lining of liver and involve in the breakdown of red blood cells also known as phagocytic cells) in the reticuloendothelial system entrapped the radio-labeled colloidal particles following an intravenous injection [19]. The particle size of radiolabeled colloidal suspensions is usually between 0.05 to 4 μm. ^{99m}Tc-macro-aggregated albumin and ^{99m}Tc-sulfur colloid are mostly used as phagocytic agents and their size ranging from approximately 0.1–2.0 μm are able to leave the circulation via the sinusoidal type capillary structures in the liver, spleen, and bone marrow [20]. There is inverse relation between particle size and its bone marrow uptake that is why the larger particles will localize in spleen and liver.

The diameter of capillary is about seven micro-meters which is larger than particle size, capillary blockade does not occur. Opsonin (serum specific protein) may interrelate and provide coating to the colloids so that may be recognize by receptors site; then, engulf and removed from circulation by cells of the reticuloendothelial system as shown in **Figure 3** [21].

Macrophages in liver sinusoids (Kupffer cells) and macrophages in spleen (reticular cells) accumulate the particles by phagocytosis. In a liver scan with ^{99m}Tc-sulfur colloid cold lesions identified may be due to intra hepatic tumor displacing normal distribution of reticuloendothelial system's cells. Similarly, decreased reticuloendothelial system functioning may appear as radiation damage in bone marrow and liver shown as cold areas in scan results. Patients having melanoma and breast cancer, ^{99m}Tc-SC has been widely used in lympho-scintigraphy for the identification of sentinel node which is the first lymph node to receive lymphatic drainage from tumor cells [22].

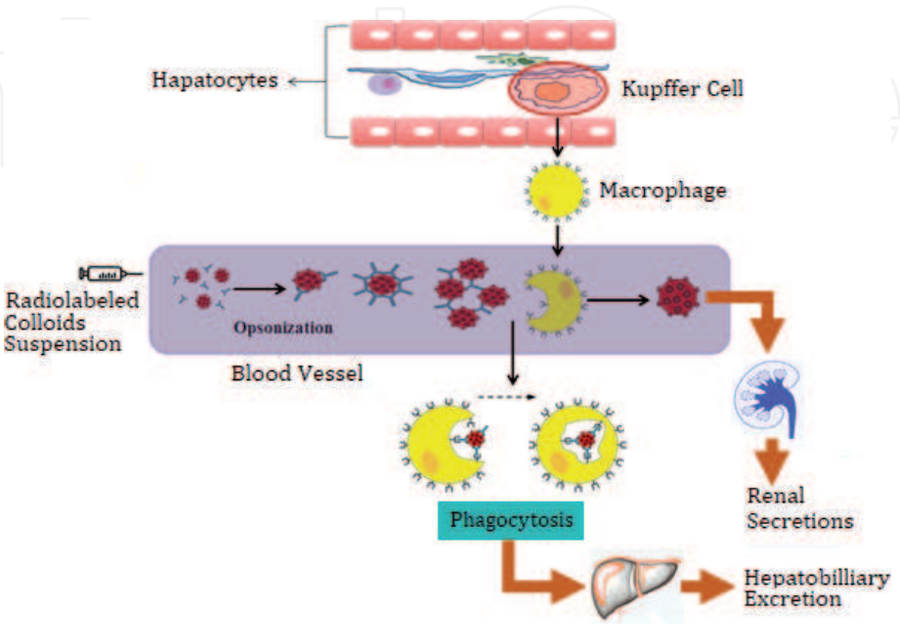

Figure 3.
Phagocytosis process through macrophages of liver (Kupffer cells) present in the lining of liver [20].

Distribution in the endothelial system is typically Five percent in marrow, Ten percent in spleen and eighty-five percent in liver. The t_{biol} of macro-aggregated albumin is 6–12 hours which is infinitely short as compared to t_{biol} of ^{99m}Tc-sulfur colloid in the liver. T ½ of clearance from the blood pool is 2.5 min; so, in approximately ten minutes only 6% remains in blood stream. Imaging must begin after 5–10 minutes of intravenous colloidal injection [23].

The radiopharmaceutical, Tc-99 m sulfur colloid, is localized by this mechanism used for liver scans. Cyst, tumor abscess or hemangioma are focal areas of lacking phagocytic cells will be demonstrated as "Areas of lack uptake". There will be a colloid shift if liver is poorly functioning such as with cirrhosis or hepatitis [22, 24].

2.4 Capillary blockade

This technique most precisely depends upon the phenomenon of micro-embolization (trapping the radiolabeled particles in the capillary bed) used to determine perfusion of organ such as brain, heart, and lung. For pulmonary perfusion studies commonly used radiolabeled particles is Technetium labeled macro aggregated albumin particles. ^{99m}Tc-MAA particles have diameter of about 10–50 μm while, pre-capillaries and capillaries have a mean diameter of 20–25 μm and 8 μm, respectively. Therefore, intravenous injection of ^{99m}Tc-MAA particles block the blood flow to the distal region of lung by physically trapped in arterio-capillary beds as shown in **Figure 4** [19, 25].

Smaller particles pass through the pulmonary capillaries and are extracted by the reticuloendothelial system in the body. Therefore, the mechanism of localization of particles in lungs is purely a mechanical process, called capillary blockade. In experimental animal studies, gold standard for determination of organ perfusion is radiolabeled microspheres with varying particle diameter and physical half-lives [27].

The first encountered capillary beds are the lungs when such sized particles injected intravenously. For perfusion lung scan radiolabeled particles (Tc-99 m

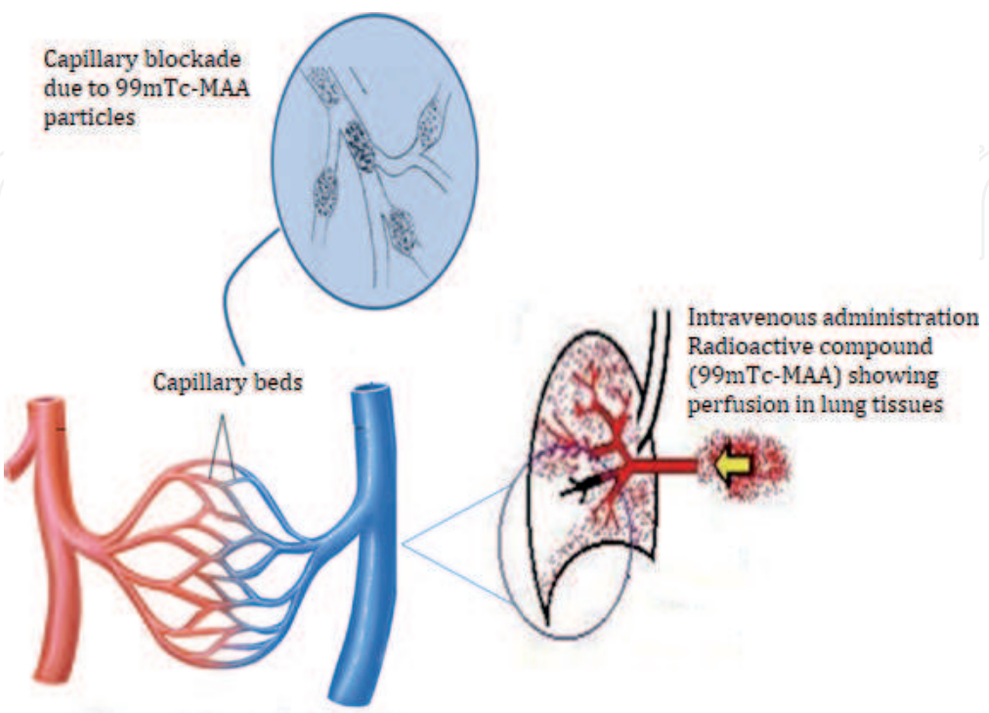

Figure 4.
Illustration of capillary blockade due to ^{99m}Tc-MAA accumulation in capillary beds [26].

macro-aggregated albumin) have been used. This delivery mechanism necessarily involves to the capillary beds via blood flow, localization of Tc-99 m MAA is a surrogate for relative blood flow in lungs. Therefore, this perfusion lung scan with Tc-99 m MAA aggregates also used to assess blood flow in pulmonary arteries. A similar procedure in which Tc-99 m MAA is injected in hepatic artery through a catheter, it is delivered via hepatic blood flow to the capillaries in the liver [19, 28].

2.5 Cell sequestration

Potentially saturable mechanism that is mostly associated with spleen and refers to the process where damaged and old RBC's removed from circulation [29]. It is unlikely for the relatively small numbers of cells used for imaging. The radiopharmaceutical preparation is carried out by in vitro labeling of red blood cells with technetium-99 m using modified Brookhaven labeling method and then damaging them by heating at 49°C for fifteen minutes (**Figure 5**).

2.6 Ion exchange

Ion exchange is a mechanism of localization in which ions exchange between a complex like hydroxyapatite and electrolyte solution. ^{18}F radioisotope is typically used for imaging metastatic and primary tumors present in bone. In ^{18}F-NaF the mechanism of localization followed by this radiopharmaceutical is Ion exchange mechanism and is used for studying metabolism of bones and also for bone imaging [19]. ^{18}F obtained from cyclotron is diluted by using 5 mL of sterile water and then passed through a sealed unit containing cation exchanger and then anion exchanger. To obtain ^{18}F-NaF, 10 ml saline (NaCl) is added in anion exchanger. And then eluted ^{18}F-NaF from anion exchanger is ready to inject in patients. The localization mechanism of ^{18}F-NaF in infected area involves the exchange of fluorine anion (F^-) from hydroxyl group (OH^-) in hydroxyapatite a bone crystal [Ca_{10} $(PO_4)_6$ $(OH)_2$]. After the exchange of F^- with OH^-, fluoroapatite [Ca_{10} $(PO_4)_6$ $(F)_2$] is formed as shown in **Figure 6** [1].

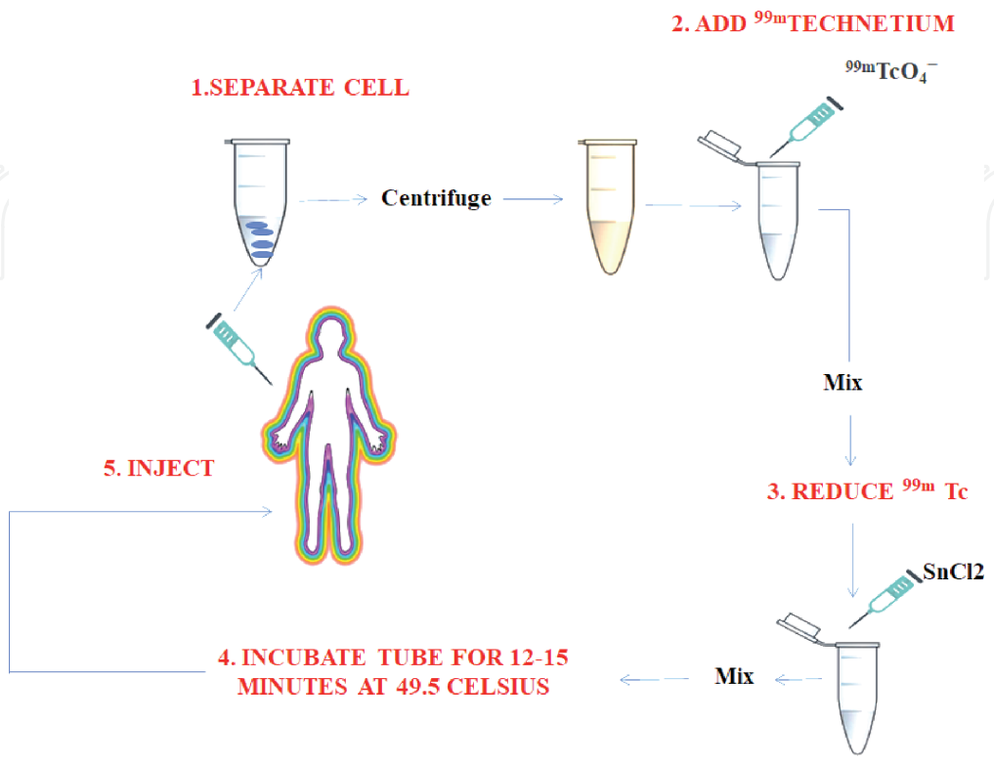

Figure 5.
Schematic explanation of ^{99m}Tc-DRBC preparation [30].

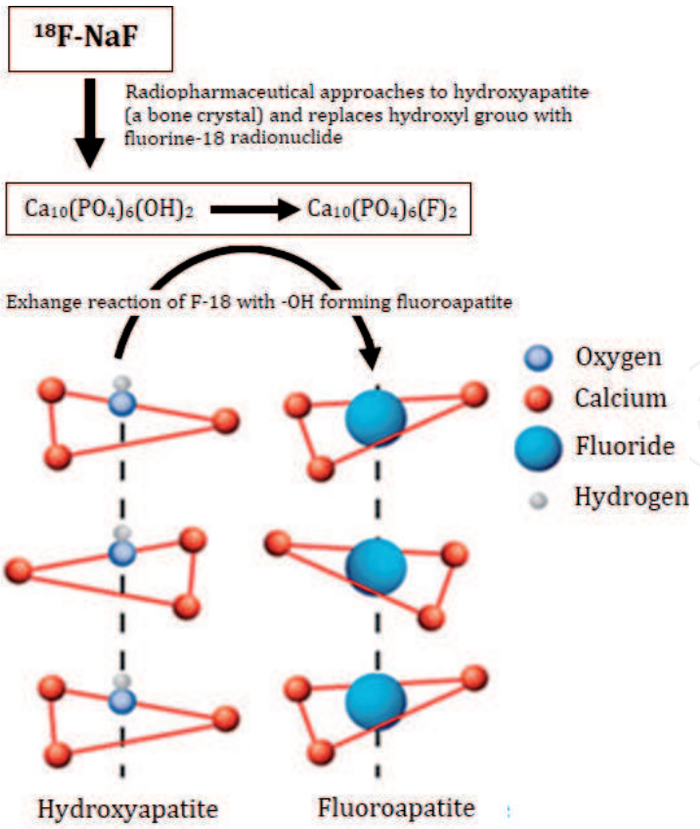

Figure 6.
Ion exchange mechanism of ^{18}F-NaF for bone deposition [31].

When ^{18}F-NaF injected in the body of patient its distribution depends on the blood flow of body and the amount of ^{18}F-NaF distributed in different bones at different ratio. In bone marrow the uptake of radioisotope is almost negligible. ^{18}F-NaF can easily diffuse through membrane and almost 30% radiotracer present in erythrocytes. ^{18}F-NaF has a fast plasma clearance rate. For bone deposition ^{18}F-NaF must pass through extracellular fluid with the help of plasma. The incorporation of fluoroapatite in bone in a slow process and it depends on the area of infected bone. In case of malignant bone disorder, the incorporation time of fluoroapatite is high. Fluoroapatite has low binding with plasma protein and rapidly clear from non-targeted area. After 40–45 minutes of radiotracer injection, fluoroapatite permits the whole body imaging [32].

2.7 Chemisorption

Chemisorption also known as physiochemical adsorption is localization mechanism refers to the binding of phosphate-type compounds like methylene diphosphate (MDP), pyrophosphate (PYP) and hydroxy diphosphate (HDP) onto the bone surface. So, with the increase in bone metabolism like tumor, fracture and infection, surface area increases and hence there is enhanced accumulation of radiopharmaceutical at that surface. ^{99m}Tc-MDP, ^{99m}Tc-PYP, and ^{99m}Tc-HDP all bind to tissues of bone by this mechanism [19].

The administration of radiopharmaceuticals with low-energy photons that are attached chemically to moiety having affinity with hydroxyapatite a bone mineral. This attachment permits selective radiation dose to the area of interest with no or minimum radiation dose to the non-infected tissues. Out of 100%, only 40–50% dose of injected radiopharmaceutical localizes in bone and the remaining 50–60% dose is excreted from body through kidneys. Since, the

radiopharmaceutical uptake in bone is low, so imaging starts after three hours of post injection [33].

2.7.1 Chemisorption mechanism of ^{99m}Tc-PYP

^{99m}Tc-PYP is used for the acute myocardial infarction imaging is an example of Chemisorption mechanism of localization. Myocardial infarction starts when myocardial cells turn out to be necrotic, calcium ions influx create into the cells. Circulating phosphate ions present in body reacts with the Ca^{2+} ions and $Ca_3(PO_4)_2$ crystals are formed. Resulting calcium phosphate crystals formed hydroxyapatite present on bone tissues. ^{99m}Tc-PYP binds irreversibly and avidly to calcium phosphate crystals at the infarct periphery where some perfusion is maintained as shown in **Figure 7**. After two hours of post injection imaging takes place [34].

2.8 Filtration

Filtration is denoted as a significant case of diffusion in which carrier molecules are compelled to progress by an osmotic or hydrostatic pressure gradient through several channels and pores. The significant example of this process explained is by glomerular filtration of kidney. Radiopharmaceuticals are effectively employed in renal imaging and in the determination of renal morphology or renal functioning. Two physiological mechanisms such as glomerular filtration and tubular secretion are accountable for renal imaging. Agents cleared by glomerular filtration are further utilized in investigating the glomerular filtration rate (GFR) [19].

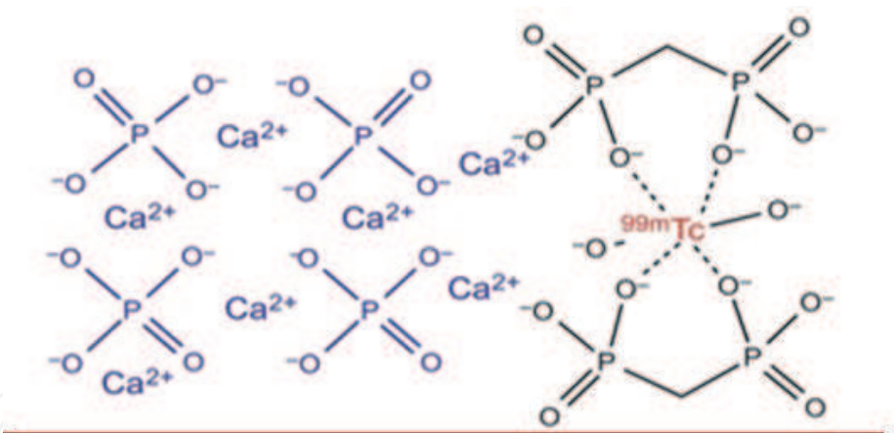

Figure 7.
Systematic representation of chemisorption of ^{99m}Tc-PYP [35].

There are two factors that are primarily concerned for the glomerular filtration of kidney comprising radiopharmaceuticals. First factor is the availability, only those molecules are liable for filtration that are freed in plasma and are not protein bounded. Second factor required for glomerular filtration is the pore size versus molecular size. Usually, only small hydrophilic molecules having a size less than 5000 are capable of disseminating through glomerular pores [36].

Some other factors are also involved in this glomerular filtration mechanism. Some pressure gradient or force is necessity for filtration while in the case of glomerular filtration, this specified force is provided by blood pressure however it does not demand any indigenous involvement of external output or energy. Moreover, filtration is non-selective due to the non-involvement of any receptors, transporters or carrier molecules [37].

Various radiopharmaceuticals are excreted partially by glomerular filtration, but the radiopharmaceutical most employed for renal imaging glomerular function is Tc-99 m DTPA. Renal DTPA can be determined from estimating the activity in multiple or single blood samples, the elimination of activity from tissue or blood and from the emergence of tracer particles in urine [19]. Example of Filtration process is depicted as shown in **Figure 8**.

Some other radiopharmaceuticals excreted indigenously during glomerular filtration are ^{99m}Tc- MAG3 and EC (ethylene di-cysteine) for tubular secretion, ^{131}I and ^{123}I for Tubular (80%) and glomerular (20%), ^{99m}Tc-DMSA for cortical binding (50%), and ^{99m}Tc-GHA for cortical binding (20%) and glomerular filtration (80%) as shown in **Figure 9**.

2.9 Active transport

Active transport is carrier mediated, metabolic, energy dependent pathway in a body to move forward a radiopharmaceutical across a cell membrane into a cell. The energy utilized during this reaction comes from ATP that allows the transport of molecules against a concentration gradient. It is carrier selective, which explicates fitting of small number of molecules into a specific carrier and makes it possible to accomplish saturation i.e. maximum response provided when all the carriers are engaged [19].

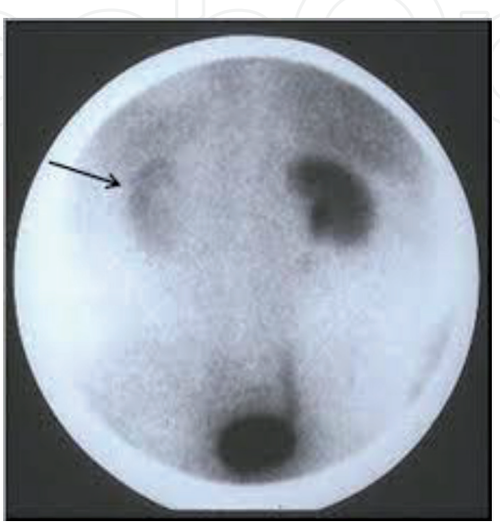

Figure 8.
Pre-treatment was done with captopril (an ACE inhibitor used for decreasing pressure on blood vessels), glomerular filtration of Tc-99 m DTPA is decreased as seen in the left kidney (arrow). Captopril employed, blocked the compensation mechanism triggered by left kidney ensuring a decreased pressure in the left kidney [19].

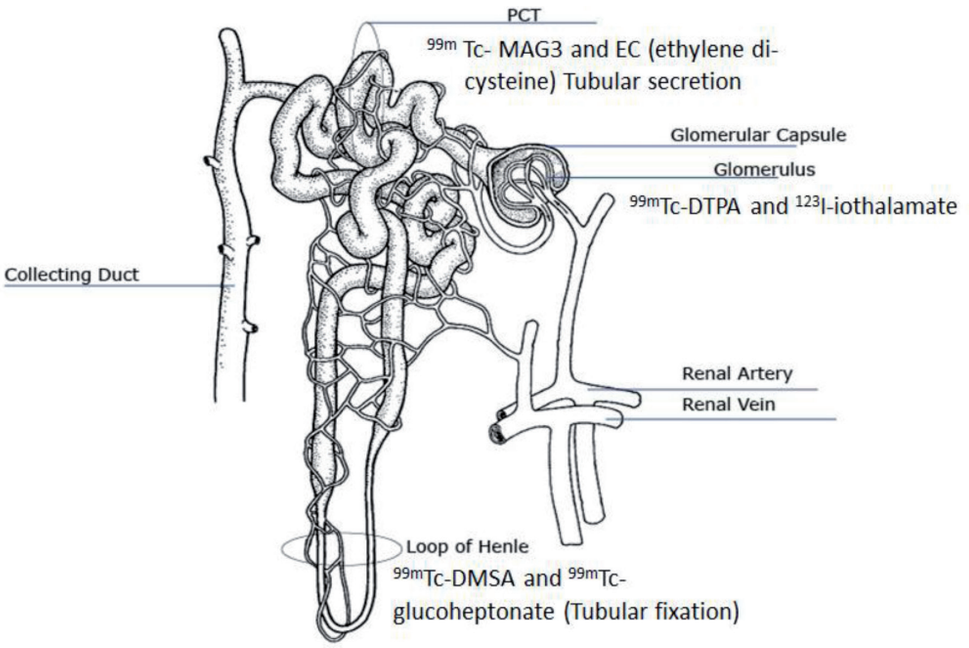

Figure 9.
Different mechanism of renal radiopharmaceutical excretion and uptake, including glomerular filtration, cortical binding and tubular secretion [38].

Concentration of iodide in the thyroid gland is an eminent example of active transport. Iodide ions are conveyed into thyroid cells by the Na^+/I^- symporter. Therefore, I-123 and I-131 (radioisotopes of iodine) are suitable radiopharmaceuticals to assess thyroid functioning [3]. Furthermore, Tc-99 m pertechnetate has almost same negative charge and ionic radius, hence it is too transported like iodide as shown in **Figure 10**.

It is highly significant that high concentrations of iodide (in the form of injections of iodinated contras media) in the blood, will competitively prevent thyroid uptake of these radiopharmaceuticals. Firstly, iodide is trapped producing an intermediate thyroglobulin and is eventually converted into T3 & T4. Preliminary, localized in thyroids, parotids and stomach and ultimately cleared through kidneys as shown in **Figure 10** [39].

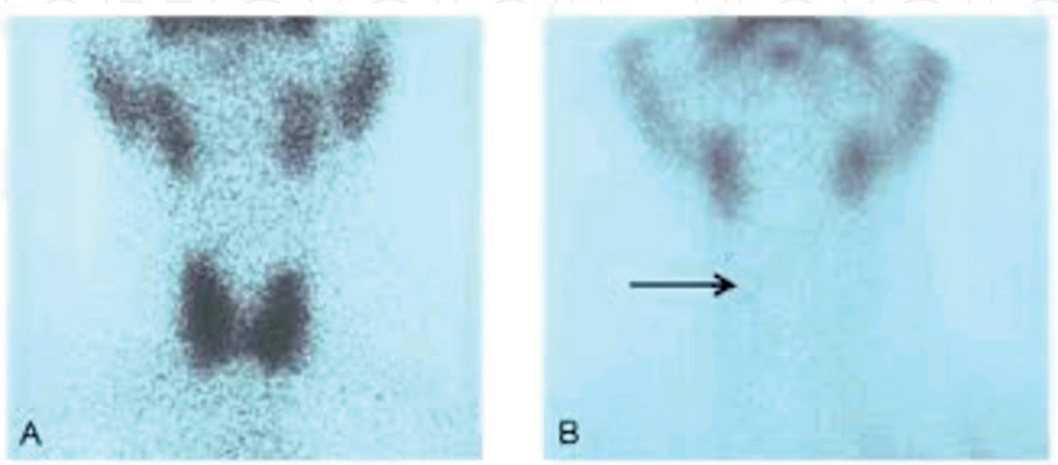

Figure 10.
(A) Regular uptake of Tc-99 m pertechnetate in thyroid (and salivary glands). (B) Absent uptake of thyroid (arrow) of Tc-99 m pertechnetate in an iodinated x-ray contrast media administered patient a few days earlier [19].

Glucose absorption from the GI tract into the blood and then reabsorption of glomerular-filtered glucose back into the blood by the distal renal tubules is another example of active transport. A sodium-dependent glucose cotransporter (SGLT) is employed to perform this function. Even though F-18 FDG is not voluntarily transported by SGLTs, glomerular filtered F-18 FDG residues in the urinary tract and flows to the bladder. Eventually, F-18 FDG do not perform the same function as glucose that is being reabsorbed into the blood [19] (**Figure 11**).

A third example of active transport is the Na+/K+ (sodium/potassium) pump, due to its significance in the heart muscle. Thallous chloride has extensively employed for myocardial perfusion scans. However, due to similar ionic size of thallous ion as potassium ion, it fits in place of potassium ion in sodium/potassium pump. Therefore, heart muscles reflect coronary perfusions.

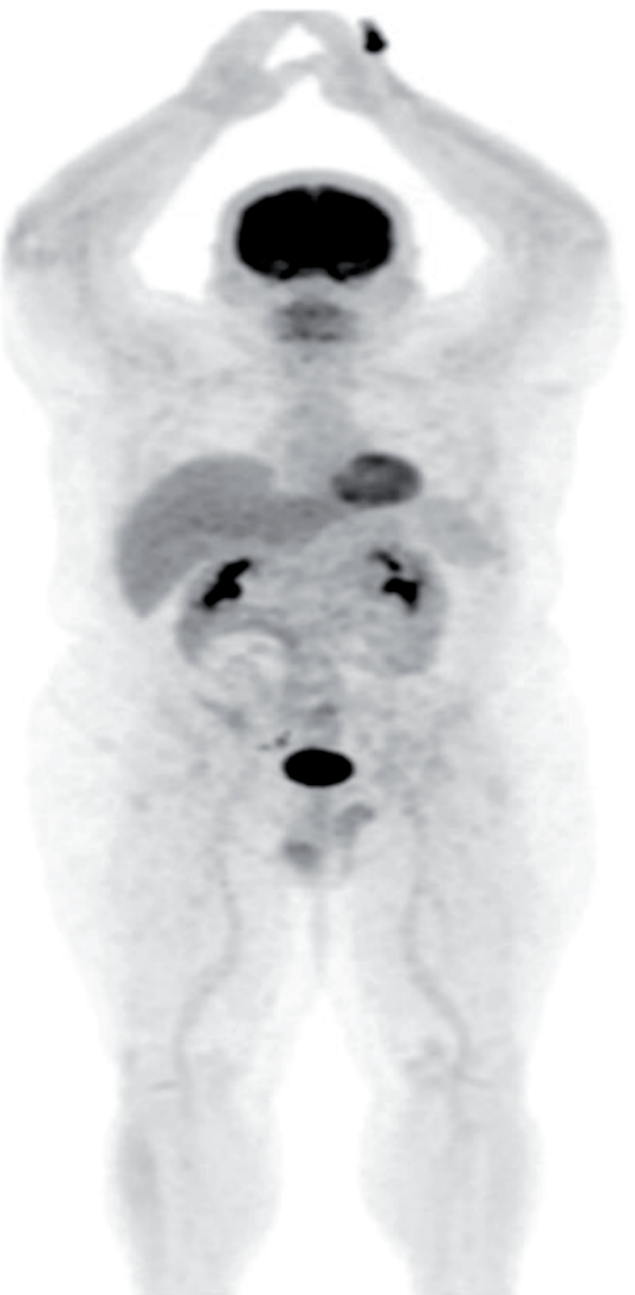

Figure 11.
Following injection of F-18 FDG in a normal patient, there is high uptake in brain, variable uptake in heart (high uptake in this patient), and moderate uptake in liver, GI tract, and marrow [19].

A second radiopharmaceutical is rubidium chloride which falls just below the potassium in periodic table has somewhat similar properties and fits in sodium/potassium pump, thus utilizing for PET myocardial perfusion scans [39].

2.10 Facilitated diffusion

A type of carrier-mediated transport across membranes is known as facilitated diffusion. Essentially, a carrier is utilized to carry the molecule across the membrane so, it is a selective carrier membrane (i.e., only certain molecules fit into the carrier). Consequently, it is inhibited by the presence of similar molecules that also fit into the carrier. Saturation can be achieved to maximum due to limited number of carriers. Facilitated diffusion expends passive so it entails a concentration gradient for its functioning. However, external energy is not employed in facilitated diffusion.

Glucose is the key example of facilitated diffusion. Glucose move into the cells by transmembrane protein transporters [GLUT]. Similarly, radiolabeled analog of glucose F-18 fludeoxyglucose (FDG), goes into the cells via the glucose transporters [GLUT]. After entering the cell, both glucose and FDG are phosphorylated by hexokinase. Glucose-6-phosphate then enters the glycolytic pathway. But the metabolism of FDG-6-phosphate is further blocked, so FDG is reserved in the cells. It is significant to summon up that glucose and FDG are competing for GLUT transporters, consequently prominent blood levels of glucose will reduce the cellular uptake of FDG [19] (See **Figure 12**).

2.11 Cellular migration

A physiological migration directed by cell especially in response to some stimuli. The principle example is taxis of WBCs in response to inflammatory chemokines and cytokines. Ex-vivo labeling of ^{99m}Tc-HMPAO and ^{111}In-oxyquinoline with phagocytic

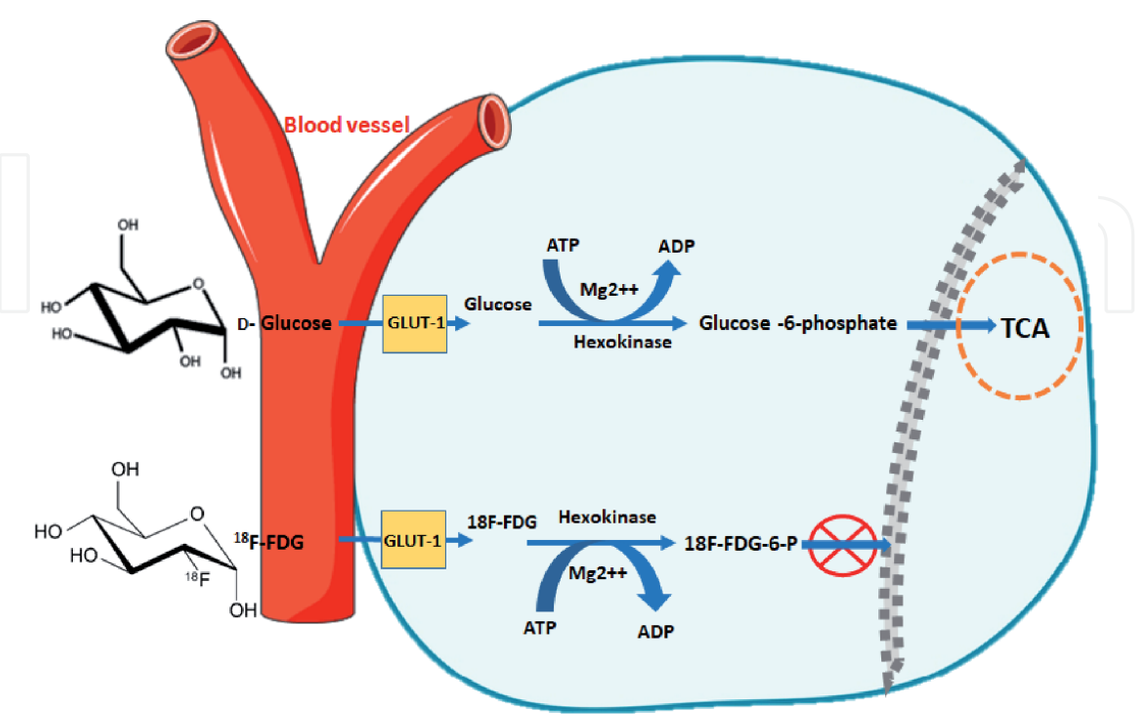

Figure 12.
Glucose and FDG transported inside cell, phosphorylated by hexokinase. ^{18}F-FDG-6-phosphate did not metabolized further but glucose-6-phosphate continue metabolism in cell mitochondria. Tumor cell, ischemic myocytes and macrophage acquired more ^{18}F-FDG [45].

leukocytes (mainly neutrophil) are frequently used complexes for infection and sterile inflammation site studies. Physiologically, autologous leukocytes chemotactically migrate towards pathogens in fact studies extended the use of leukocytes for radiolabeling that not only invade pathogens but also diagnose infection foci. At least 2000 or more leukocyte per microliter should be labeled for better quality image [40]. Labeled leukocytes were mostly neutrophil so that these complexes more sensitive to the neutrophil mediated infections. The uptake and rate of migration of radiolabelled cells depends upon the site of infection, virulence, stage of infection, kind of pathogen, upon antibiotic therapy and angiogenesis of tissues [41].

Ex-vivo labelling of ^{111}In- oxyquninoline with leukocytes was initiated by McAfee and Thakur [42]. The ^{111}In-oxine was neutral, lipid soluble, non-specific blood cells labeling agent that passively penetrate through bilayer membrane and bind with cytosol component (lactoferrin; iron bounded protein released by neutrophil). The lactoferrin bind with indium more firmly than oxine and free oxine (8-hydroxyquinoline) leave the cell environment. Scintigraphy using ^{111}In-oxine (8-hydroxyquinoline) with labeled leukocytes (WBCs) were the clinically proved agent of choice for detecting infection foci accurately [43, 44].

Approximately after 1 hour of injection, about 60% radioactivity of indium labeled leukocytes were found in the lungs and if not damaged migrate to liver, spleen, bone marrow and reticuloendothelial system. In case of infection, radiolabeled WBCs accumulate at the site of infection due to chemotactic attraction of biofilms and other soluble products of bacteria. The reason for the regular usage of ^{111}In- leukocyte for tumor imaging were its stability, normal body distribution and complementary bone marrow imaging as shown in **Figure 13**. The cons of complex are its lower sensitivity in infection that cannot elicit the neutrophil response e.g. tuberculosis and about 18 to 30 h delay in injection administration and imaging [40].

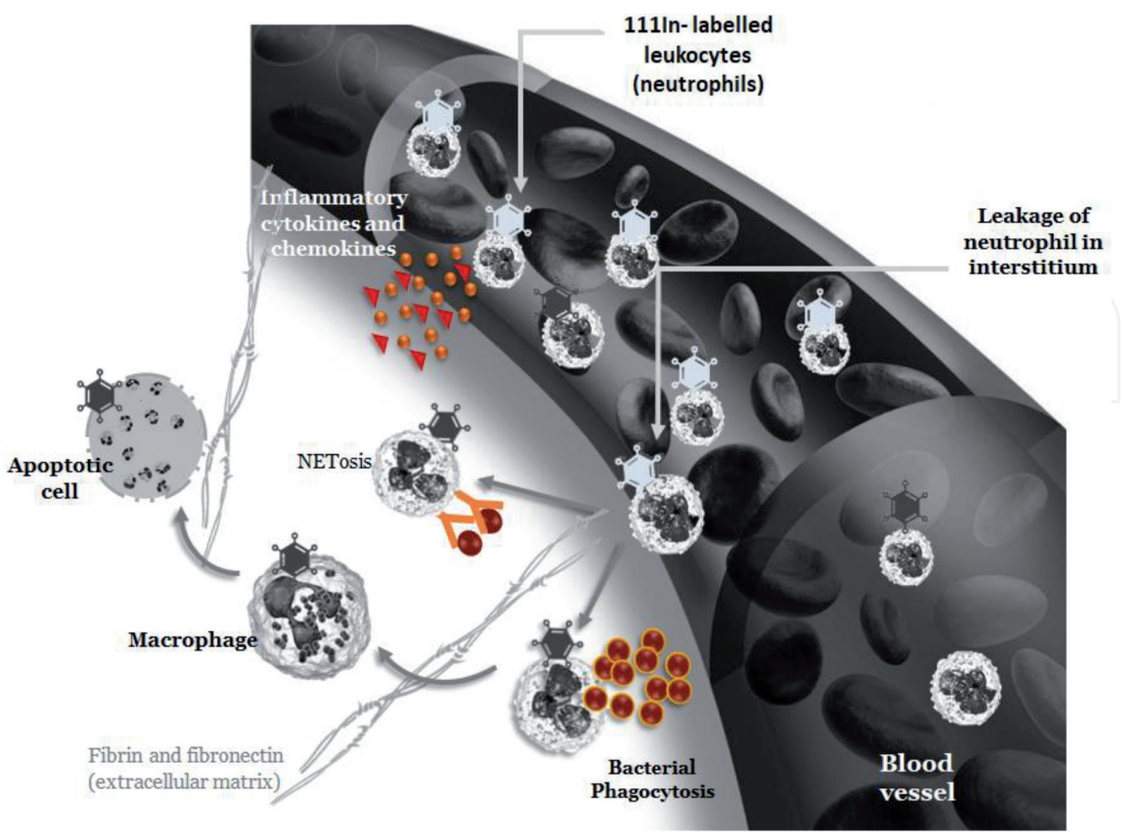

Figure 13.
Depiction of tumor cell microenvironment. ^{111}In-oxine labeled with leukocytes. Leukocytes move within blood stream and act as first line of defense. Attached radiotracer (^{111}In) image tumor cell microenvironment [45].

^{111}In-oxine labeled leukocytes preferably practiced for the diagnosis and therapy of inflammatory bowel disease, osteomyelitis, abdominal infection, diabetic foot, vascular prosthesis, pelvic sepsis, lung infection, fever of unknown origin, neurological infection, and endocarditis etc. Furthermore, for the ex-vivo radio-labeling sterile conditions should be taken because there was a possible risk of cross contamination that may be tainted with hepatitis B, C or HIV.

^{99m}Tc- exametazime (HMPAO) labeled with autologus leukocytes (predominantly neutrophils) follow the same pathway for infection and inflammation imaging as ^{111}In-oxine labeled leukocytes. Neutrophil, an important part of our innate immune system moved towards acute infection foci and invade pathogens [45]. Labelling of leukocytes followed by intervenously administration of radiolabelled complex, due to inflammatory cytokines and chemokines; WBCs were attracted towards infection site. The ^{99m}Tc-leukocyte detect abnormalities soon after the injection and image not only reticuloendotelial system but also visualize urinary tract, bowl and gall bladder. Limitation includes the short half life of ^{99m}Tc and delayed bone marrow imaging (2 to 3 days between leukocyte imaging and bone marrow imaging) [40].

Platelets; an important part of thrombus formation, when **labeled with ^{111}In** can follow simple cell migration mechanism to incorporate inside active thrombus formation so that easily picturize the thrombus formation**. Heat damaged ^{99m}Tc-RBCs** taken up for the examination of splenic nodule tissue formed after splectomy. During circulation of old and new RBCs, the old and damaged one was sequenter in the spleen. In same way heat damaged labeled RBCs sequenter inside spleen and imaged accessory spleen tissues [45].

3. Infection imaging agents based on metabolic activities

Tumor cells have higher metabolic rate as compare to the normal body cells, this upreglate the metabolism of cells and trap more molecule per gram than normal somatic cells. Through different metabolic ways like enhanced glucose metabolism for harvesting more energy. Following mechanism involved in proliferating cell metabolism and

- Sugar metabolism
- Iron metabolism
- Amino acid metabolism
- Lipid metabolism
- Thymidine kinase activity and folic acid synthesis
- Imaging cell micro-environment through Hypoxia and acidic pH

3.1 Sugar metabolism

Cancerous cells proliferate rapidly and get more energy to fulfill physiological activities. Glucolysis is the preliminary energy driving metabolism. What would happen if the same metabolism used for imaging cell?

3.1.1 Deoxyglucose

An analogous molecule of glucose but not sugar it has one oxygen atom less than glucose. Fluorine (F- 18), a cyclotron based radionuclide labeled with glucose analogous (deoxyglucose) through nucleophilic reaction with mannos triflate (precursor) [2]. **^{18}F-FDG (fluorodeoxyglucose**) practice for clinical oncology since 1980s [46]. The fluorodeoxyglucose participate and transport inside cell by following the same pathway as glucose through glucose transporter; GLUT-1. This glucose transpoter GLUT-1 release in stress condition and a member of glucose regulating protein [45]. As said earlier deoxyglucose is a glucose analogous, so this analogous molecule metabolized by the same pathway as glucose and was trapped in place of glucose molecule and get phosphorylated (glycolysis) as shown in **Figure 12**.

Glucose-6-phosphate further participate in glycolysis but FDG-6- phosphate cannot metabolized (not being the subsequent substrate) as glycolytic enzyme glucose-6-phosphate isomerase (hexokinase) has strict structural and geometric demands so fluorine substituted; 2-oxy-2-fluoro-D-glucose trapped and accumulate inside cell cytoplasm (metabolic trapping) [44]. Remember that glucose and FDG compete for the same transporter GLUT-1, so higher glucose level may lower the uptake of FDG. The enzyme hexokinase may convert back fluoro-6-phosphate to FDG but cancerous cell have very low amount of this enzyme so this trapped molecule (^{18}FDG-6-PO_4) aid in-vivo study of homeostatic system without disturbing their function. ^{18}F-FDG is presently the most widely used PET tracer for imaging non-invasive malignant tissues that highly metabolized glucose [45].

The ^{18}F-fluorodeoxyglucose participate in imaging of osteomyelitis, spinal infections, endocarditis, infected joint prosthesis, diagnose FUO and diabetic foot infection. Limitation regarding ^{18}F-FDG use that it cannot differentiate between infection and sterile inflammation.

3.1.2 Sorbitol

Another alcohol soluble sugar; **sorbitol**, act as a metabolic substrate for bacterial specific imaging. Gram negative bacterial strains (*Klebsiella pneumoniae*, *Escherichia coli*, Yersinia pestis, Enterobacter spp., etc.) show promising findings but limited detection in case of Gram-positive bacteria and mammalian cancer cells. Sorbitol was taken up by the bacterial surface membrane transporter, then phosphorylated and metabolized in the same manner as glucose. Initially ^{18}F-FDG reduce to ^{18}F-FDS (fluorodeoxysorbitol) as shown in **Figure 14** than transported to bacterial cell environment where analogous glucose metabolism begin next [47]. Interesting fact is that mammalian cells did not have transporter for this sugar [43]. Moreover, ^{18}F-FDS act as promising agent in PET imaging for monitoring efficacy of antibacterial burden and proved to be safe for intravenous human use that determine radiation dosimetry and cell biodistribution [48].

3.2 Iron metabolism

For the development of new radiopharmaceuticals similarities with ferric ion (Fe^{+3}) was very important as iron is a fundamental part of our body and many iron binding proteins likewise transferrin, lactoferrin and ferritin transport and store iron in-vivo. $^{67}Ga^{++}$ ion produced at physiological pH its infection uptake is multifactorial since it shares similar chemical characteristic and biodistribution properties with ferric ion (Fe^{+3}). When ^{67}Ga- citrate administrated in blood plasma due to the increase cell permeability and blood flow about 90% activity exchange ligand

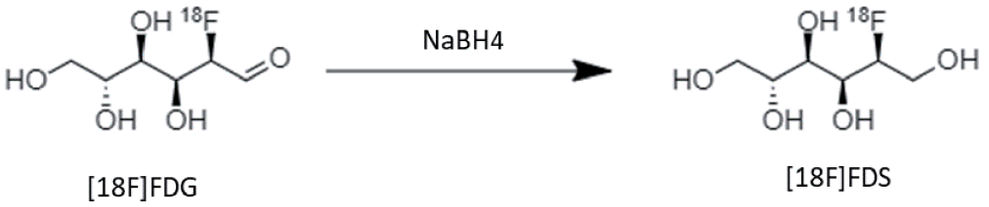

Figure 14.
Reduction reaction of 2-Deoxy-2-[^{18}F] fluoro-D-glucose to 2-Deoxy-2-[^{18}F] fluoro-D-sorbitol using $NaBH_4$ reducing agent.

with plasma protein in extracellular space. Therefore, iron atom always competes with radio-metal (^{67}Ga) for binding with plasma protein. ^{67}Ga-citrate exchange ligand with transferrin protein in cell plasma. Cancerous cells overexpress cell proliferation and metabolic activities, to meet the cell membrane receptors demand tumor and inflammatory cell membranes have ubiquitous membrane receptors on them. In fact, infinite transferrin receptors are getting to the cell having rapid cell growth and upregulated DNA synthesis (like tumor and inflammatory cells), thus ensuring more uptake of $^{67}Ga^{++}$.

^{67}Ga-citrate localize non-specifically at the site of infection where the ^{67}Ga-transferrin complex formed due to the leakage of plasma protein from blood vessel to extracellular space of inflamed tissues. The acidic environment of inflammatory interstitial tissue space has more lactoferrin another plasma protein secreted by stimulated or dead neutrophils, which subsequently tie with ^{67}Ga due to higher ionic attraction [2]. Another ^{67}Ga uptake mechanism seen in bacterial infection, a ^{67}Ga-avid, direct attachment of ^{67}Ga with bacterial siderophores (specific prokaryotic metal chelating peptides) [49]. Some gallium atoms also transported by circulating WBCs [40].

^{67}Ga-citrate used primarily for the diagnosis of spondylodiskitis, moreover for benign and neoplastic lymphomas particularly in evaluating staging, prognosis and follow up imaging of residual disease. Though ^{67}Ga-citrate not being specific for bacterial infection and replaced with ^{18}F-FDG/PET but still ^{67}Ga-citrate are widely used to identify the site of FUO and worthwhile in nuclear oncology (Hodgkin's and non- Hodgkin lymphoma) [2, 43, 50]. Disadvantages of ^{67}Ga may include its short physical half-life ($t_{1/2}$ = 68 min), uptake in inflammation and trauma [40].

3.3 Amino acid metabolism

Amino acids and proteins are the key elements in building block of life. Amino acid actively transport and uptake greaterly in the proliferating cancerous cells which reflects the increase synthesis of protein. Methionine, an essential natural occurring amino acid customize as l-[methyl-^{11}C] methionine and potentially used in PET oncology. Additionally tyrosine, another essential amino acid analog frequently used as radiolabelled tracer. As these tyrosine tracers not involved in protein synthesis [^{11}C] methyl-1-tyrosine,O-(2-[^{18}F] fluoroethyl)-L-tyrosine (FET), 1-[2-^{18}F] flourotyrosin, 1–4-[^{18}F] fluoro-m-tyrosin and 1-[3-^{18}F]-a-methyltyrosine (FMT), these analogs used in evaluating brain tumors, neuroendocrine tumors, prostate and pancreatic cancer uptake [45, 51, 52].

3.4 Lipid metabolism

The upregulation of glycolysis, iron and amino acid metabolism in cancerous cells also characteristically agitate the lipid production. During normal

conditions production of triglycerides combined with long term energy reservoir. Cancerous cells do not manage the cell energy requirement with primary source; carbohydrates. So they preferentially employed lipid metabolism to meet energy requirement by producing more essential membrane phospholipids and phosphatidylcholine [46]. As a result two essential lipid production enzymes fatty acid synthase (FAS) and choline kinase (ChoK) overexpressed in lymphomas including breast, lung, colon, ovarian, and prostate cancers. So in lipid de novo synthesis FAS catalyze the acetic acid reaction for the synthesis of phospholipid phosphotidylcholine and choline kinase responsible for phosphocholine production as shown in **Figure 15**. Fatty acid radiolabelled analogs [^{11}C]- Acetate, [^{11}C]-Choline, [^{18}F]-Fluorodeshydroxycholine [^{18}F]-Choline, [^{18}F]-Flouoethycholine used in PET oncology imaging of brain tumors, liver tumors, prostate and breast malignancies [53, 54].

3.5 Thymidine kinase and folic acid synthesis pathway

Thymidine kinase; a metabolic substrate that catalyze the conversion reaction of nucleoside subunits to nucleotide units and then use these units in the synthesis of DNA. These labeled bacterial substrate initialize for SPECT [^{125}I]-FIAU and PET [^{124}I]-FIAU imaging. Thymidine based PET radiotracers [^{11}C] TdR, [^{18}F] FLT, [^{18}F] FMAU and [^{76}Br] FBAU [46, 57].

Folic acid; another metabolic salvage for nucleic acid synthesis (subsequently DNA synthesis) in prokaryotes. Para aminobenzoic acid (PABA) responsible for the folic acid production in microorganism and this substrate labeled with radiotracer [^{18}F]-PABA/PET. This radiofluronated analogues [^{18}F]-PABA holds potential for clinical translation in bacteria and poor attraction with mammalian cells [58].

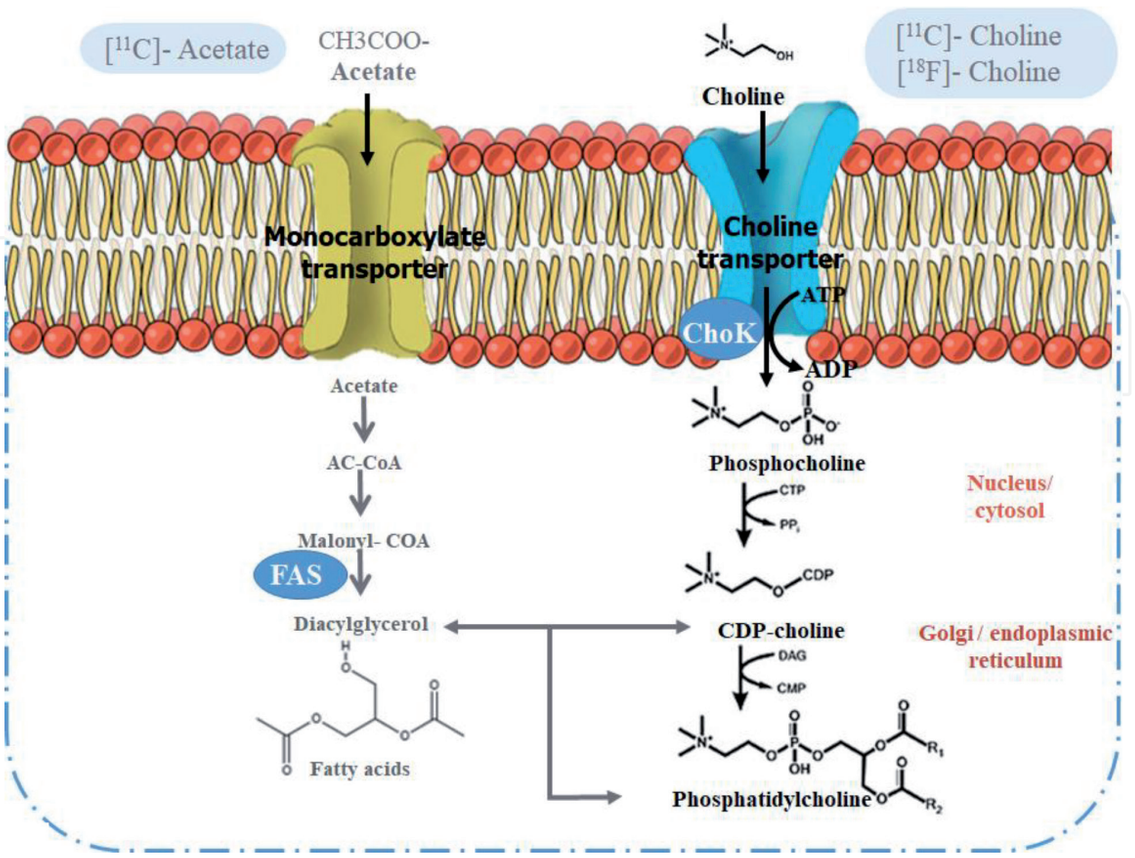

Figure 15.
De novo fatty acid synthesis mechanism using acetate substrate [55, 56].

3.6 Oxidative metabolism (tissue hypoxia)

Hyoxia, a phathophysiological condition portray deprived of adequate oxygen level in tissues. A normoxic cell have oxygen level 20–80 mmHg compared to hypoxic cell <3 mmHg. In malignancies, irregular vascularization cause ischemic hypoxia. The severity of cancerous hypoxia depend upon tumor phenotype for example cervical cancer has severe hypoxic injury. Hypoxia may alter the function in tumor microenvironment particularly angiogenesis, vasculogenisis, apoptosis and prospensity for metastasis [46].

Potential hypoxia selective PET radiotracer has been developed to evaluate tumor microenviroment.^{18}F-fluoromisonidazole (FMISO) and ^{64}Cu-[4-*N*-methyl-3-thiosemicarbazonato ligand] (ATSM) translated for hypoxia imaging [59].

4. Cell proliferation

Tumor specific radiolabeled drugs are now clinically approved for non-surgical treatment and molecular imaging of malignant growth of cells and definite modifications were implemented to make possible radionuclide therapy of cancerous cells. Uptake, delivery and retaining mechanisms of radiolabeled drugs in targeted tissues and organs involve many ways which are of particular importance [60]. Normally, cells and tissues maintain a consistency between cell proliferation and cell death. On the other side, carcinogenic cells promote cell growth. In addition, amplified mitotic rate, increased cell growth and reduced differentiation are responsible for enhanced cell propagation. Generally, progression rate of cancerous cells depends upon the differentiation levels of benign and malignant tissues that leads to advanced mitotic rates [61] (**Figure 16**).

The idea of localization of radiolabeled drugs at tumor sites is best described in terms of transformed physiology of specific proliferating cells. Such localization should take place in correlation with diseased parts of the body including external and internal regions of infected areas [63]. Tumor targeting involves a certain type of interaction between medication and its receptors at affected tissue site. Malignant tumors required excess quantity of nutrition and release certain receptors which, in contrast, used as carriers to distribute cytotoxic agents as shown in the above figure. Larger number of rapidly producing cells were compared with normal cells during cell cycle i.e. S-phase. Consequently, substrate requirement in the form of nucleotides for DNA synthesis was also increased. This nucleotide incorporation into DNA of tumor cells is determined using thymidine to measure the number of proliferated cells. ^{11}C-labeled thymidine has been utilized as PET radiotracer to image head and neck. Furthermore,

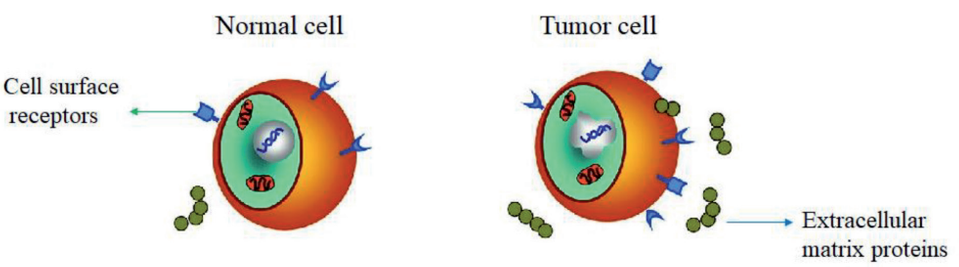

Figure 16.
Difference of cell surface receptors in normal and tumor cells [62].

targeted drug delivery systems necessitated drug localization and carriers within the desired organ.

In diseased patients, diagnosis and evaluation of therapeutic response is accomplished with positron emission tomography (PET). Studies based on this technology seek imaging mediators with eminent tumor selectivity and specificity for distinct attributes [64]. In 1950s, procedures were considered to estimate quantity of thymidine integrated into DNA of malignant tissues by using **^{3}H-Thymidine**. Meanwhile, in 1972, ^{11}C-labeled thymidine was evolved in molecular imaging to approximate cell growth. Nonetheless, rapid metabolic rate of this radiolabeled drug makes it less convenient for repetitive imaging practice.

^{18}F- 3′-deoxy-3′-fluorothymidine (FLT) is significantly developed radiotracer for molecular imaging techniques to investigate cell proliferation as it provides prolonged time interval so that there will be less quantity of labeled metabolites and scanning tissues will be cleared off catabolic waste. Transportation of FLT takes place into cell through distinct transporters and enzymatic action of thymidine kinase 1 (TK1) phosphorylated radioactive tracer into ^{18}F-FLT monophosphate that got trapped into cell. Moreover, PET images demonstrate additional phosphorylation into FLT-TP by enzyme thymidylate kinase. Reaction end products are then metabolically stuck within cells due to membrane impermeability and resistant to mortification.

FLT has greater potential to evaluate the status of malignant cells for therapeutic purposes. Diverse range of melanoma tissues i.e. breast, lung, head, neck, lymphoma and gastrointestinal have been analyzed by means of fluorine labeled thymidine [65]. Finally, ^{18}F-FLT is under evaluation and measurement of anticancer therapeutic response.

^{18}F-florouridine as a nucleoside analogue illustrates localization by cell proliferation but the radiopharmaceutical also incorporated into DNA and RNA of tumor tissues. **^{11}C-thymidine** was considered to observe multiplying tumor cells but prompted catabolic rates create hindrance in drug uptake volume and leads to complex imaging due to interfering catabolites (radiolabeled). **^{18}F-1-(2′-fluoro-2′-deoxy-β-D-ribofuranosyl) thymine (FMAU)**, a fluorine labeled analog of advanced stability with favorable results in animal cells. Phosphorylated complex incorporated into DNA to examine cell proliferation. Radioiodine I-131 & I-123 labeled **metaiodobenzylguanidine (MIBG)** represent the potent radioactive drug with diagnostic and therapeutic response to treat metastatic tumor. Even though, peptide receptors are now interchanging radiotherapy of neuroendocrine tumors, but the labeled drug still used to treat chromaffin tumors. Following ^{11}C-labeled amino acid analogs, **^{11}C-L-methionine and ^{11}C-5-hydroxytryptophane,** are used to visualize breakdown rates of cancer cells and imaging of different phases of thyroid tumors.

An analog of dihydroxyphenylalanine, **^{18}F-DOPA,** stored in brain tumor cells and exhibit amino acid transportation.^{18}F-labeled synthetic amino acids i.e. L-leucine derivatives, **^{18}F-fluoro-cyclobutyl carboxylic acid (FACBC)**, are preferentially firm and rigid with extended time frame of uptake by prostate tumor [66] (**Figure 17**).

^{18}F-fluoroethyl tyrosine (FET) localized in brain tumor cells and help to determine the type of therapeutic treatment and fate of proliferating tissues. ^{11}C and ^{18}F labeled pyrimidine analog, **2'-Fluoro-methyl-D-arabino-furanosyluracil (FMAU)** considered worthwhile for examining multiplying tumor cells. FMAU stored in the cancerous cells, phosphorylated and incorporated into DNA by enzymatic action of DNA polymerase with the potential to image DNA replication in normal and cancerous cells [68].

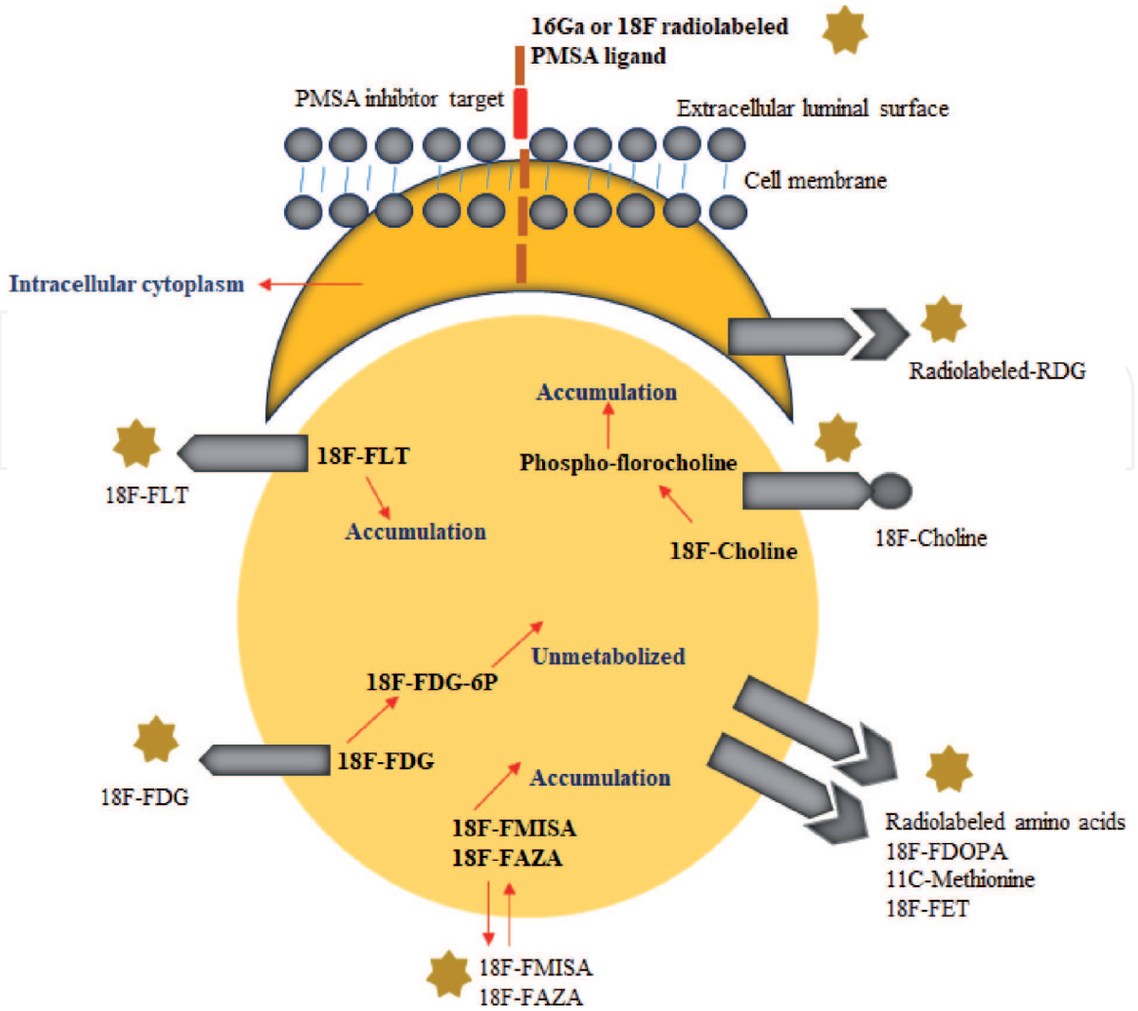

Figure 17.
Pathophysiological mechanisms of significant radiotracers used in investigation of malignant cells [67].

5. Specific receptor binding

Receptors are attachment sites for ligand molecules i.e. polypeptide hormones and neurotransmitters. In case of antigen–antibody complex formation, antigen expression on cell surface is considered a definite receptor site for antibody binding. Antigen fragments are present on the upper surface and within the cells or sometimes released into body fluids. Localization of definite receptor-binding radiotracers depends upon multiple factors such as blood clearance, affinity of the tracer & receptor and blood flow of the tumor tissue. Receptors are of various types with specificity of basic compound including peptides, steroid hormones, and antibodies.

5.1 Somatostatin receptors

Naturally, existing somatostatin (SST) complexes of peptide formation are of two types. One with 14 amino acids (SST_{14}) and other with 28 amino parts and designated as SST_{28}. In human beings, SST receptors have been recognized on cell surface of neuroendocrine region and on lymphocytes. Seglitide and somatuline are synthetically prepared somatostatin analogs with more stability than SST_{14} because the latter one join SSTR sub-types with equivalent association. To image growing SSTR cells, iodine labeled octreotide radioactive tracer pioneered the functioning of radiolabeled peptides [69] (**Figure 18**).

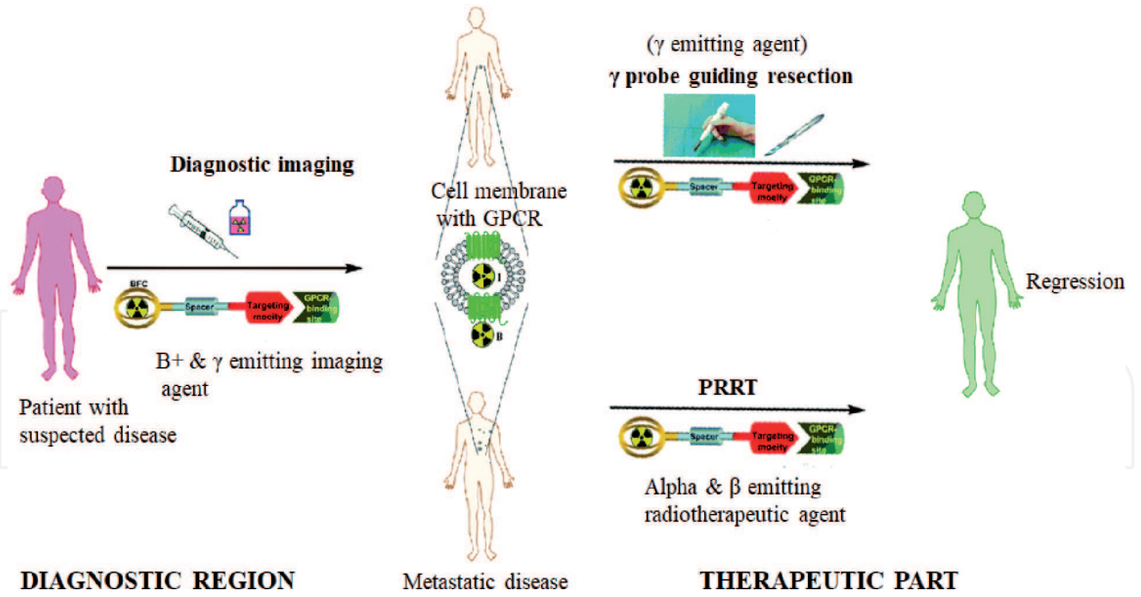

Figure 18.
Schematic representation of radiotheranostics using radiolabeled peptides [70].

- **^{111}In-DTPA-pentetreotide**was developed with specific amounts of ^{111}In (10 μg) but showed short residing time as released from body circulation via kidneys (approximately 50% in 5 h). After that, **^{90}Y-DOTA-octreotide** was formed with the similar capacity to bind proliferating cells revealing SSTR type 2.

- **^{99m}Tc-P829 peptide** exhibited peculiar binding ability with SSTR types showing the potential to image rapidly growing cells. The radioactive product is FDA approved to image lung cancerous cells [71].

5.2 Vasoactive intestinal peptide (VIP) receptor

A 28 amino acid neuroendocrine moderator with diverse variety of biological activity in various cells and tissues. Although, receptors of cell membrane are extensively present along gastrointestinal tract. However, few receptor cells found on adenocarcinomas, malignant tumors, neuroblastomas, and pancreatic cancerous cells.

^{123}I-VIPwas formulated with extraordinary activity ratio of radionuclide of about 200 MBq/μg of product to be specifically localized in liver, lung, pancreatic and gastrointestinal malignant cells [72].

5.3 Steroid hormone receptor

Steroid chemicals such as estrogen and progesterone have high binding affinity with intracellular receptors which are used to identify hormone dependent proliferating cells in case of breast cancer. Various types of hormonal analogs radiolabeled with PET imaging radiotracers. **^{18}F-fluoro-estradiol (FES),** with specificity for estrogen hormone, has revealed greater potential for analyzing metastatic tumor cells. **^{123}I-methoxy-iodovinylestradiol** (radioactive ligand) was used to diagnose estrogen receptors in breast carcinogenic cells [73].

5.4 Low density lipoprotein (LDL) receptors

Plasma lipoprotein transports cholesterol towards adrenal gland that act as the substrate for synthesis of steroid hormone. **^{131}I-iodomethyl-norcholeterol**

(NP 59) used to identify patients suffering from adrenal cortex. Cholesterol analogs, **^{131}I-iodocholestrol and ^{75}Se-iodomethyl-norcholestrol,** are under investigation for clinical advantages to detect malignant tissues. Besides N59, various iodine labeled hormonal products are undergo transportation and localization with the help of LDL receptors. A corticosteroid, Dexamethasone, reduce cholesterol uptake by controlling the production of ACTH [74].

6. Conclusion

Accumulation of radiopharmaceuticals at diseased cells through one or variety of localization mechanisms describes the specificity and efficacy of the tracer agent. The description of different localization mechanisms in above sections, helps in developing new radiopharmaceuticals for theranostics. However, the success of the radiopharmaceutical depends on the accumulation of radiopharmaceutical at specific target cells in term of per cent of injected dose per gram organ or tissue. According to the survey of literature, which has been cited in this chapter, different localization processes are quite promising but the receptor based localization of radiopharmaceuticals is the most successful nuclear medicine procedure both in diagnosis and therapeutic treatments of global fatal diseases.

Author details

Sana Komal[1], Sana Nadeem[1], Zahra Faheem[1], Arouma Raza[1], Komal Sarwer[1], Hijab Umer[1], Samina Roohi[2] and Syed Ali Raza Naqvi[1*]

1 Department of Chemistry, Government College University, Faisalabad-38000, Pakistan

2 Isotope Production Division, Pakistan Institute of Nuclear Science and Technology (PINSTECH), Nilore-Islamabad, Pakistan

*Address all correspondence to: draliraza@gcuf.edu.pk

References

[1] Holland, J.P., *The Radiopharmaceutical chemistry of seldom-used radionuclides in nuclear medicine*, in *Radiopharmaceutical Chemistry*. 2019, Springer. p. 425-446.

[2] Vallabhajosula, S., R.P. Killeen, and J.R. Osborne, *Altered biodistribution of radiopharmaceuticals: role of radiochemical/pharmaceutical purity, physiological, and pharmacologic factors.* Semin Nucl Med, 2010. **40**(4): p. 220-41.

[3] Vallabhajosula, S. and A. Owunwanne, *Basis of Radiopharmaceutical Localization*, in *The Pathophysiologic Basis of Nuclear Medicine*. 2015, Springer. p. 45-68.

[4] Chamberlain, M.C. and J. Corey-Bloom, *Leptomeningeal metastases: 111Indium-DTPA CSF flow studies.* Neurology, 1991. **41**(11): p. 1765-1765.

[5] Bunker, S.R., et al., *Detection of Gastrointestinal Bleeding Sites: Use of In Vitro Technetium Tc 99m—Labeled RBCs.* JAMA, 1982. **247**(6): p. 789-792.

[6] Shaffer, E., P. McOrmond, and H. Duggan, *Quantitative cholescintigraphy: assessment of gallbladder filling and emptying and duodenogastric reflux.* Gastroenterology, 1980. **79**(5): p. 899-906.

[7] Hauser, W., et al., *Technetium-99m DTPA: a new radiopharmaceutical for brain and kidney scanning.* Radiology, 1970. **94**(3): p. 679-684.

[8] Brazil, R., *A barrier to progress: getting drugs to the brain.* Evaluation, 2020. **14**(47): p. 19.

[9] Welch, M., M. Adatepe, and E. Potchen, *An analysis of technetium (99mTcO4–) kinetics: The effect of perchlorate and iodide pretreatment.* The International journal of applied radiation and isotopes, 1969. **20**(6): p. 437-445.

[10] Ancri, D., et al., *Diagnosis of cerebral lesions by thallium 201.* Radiology, 1978. **128**(2): p. 417-422.

[11] Ancri, D. and J. Basset, *Diagnosis of cerebral metastases by thallium 201.* The British journal of radiology, 1980. **53**(629): p. 443-453.

[12] Jones, A.E., et al., *Brain scinTIGraphy with 99mTc pertechnetate, 99mTc polyphosphate, and 67Ga citrate.* Radiology, 1974. **112**(1): p. 123-130.

[13] Delmon-Moingeon, L.I., et al., *Uptake of the cation hexakis (2-methoxyisobutylisonitrile)-technetium-99m by human carcinoma cell lines in vitro.* Cancer research, 1990. **50**(7): p. 2198-2202.

[14] Arbab, A.S., et al., *Uptake of technetium-99m-tetrofosmin, technetium-99m-MIBI and thallium-201 in tumor cell lines.* Journal of Nuclear Medicine, 1996. **37**(9): p. 1551-1556.

[15] Rowe, S.P., et al., *Correlation of 99mTc-sestamibi uptake in renal masses with mitochondrial content and multi-drug resistance pump expression.* EJNMMI Research, 2017. **7**.

[16] Del Vecchio, S. and M. Salvatore, *99m Tc-MIBI in the evaluation of breast cancer biology.* European journal of nuclear medicine and molecular imaging, 2004. **31**(1): p. S88-S96.

[17] Moretti, J.-L., et al., *To use MIBI or not to use MIBI? That is the question when assessing tumour cells.* European journal of nuclear medicine and molecular imaging, 2005. **32**: p. 836-42.

[18] Hendrikse, N., et al., *Visualization of multidrug resistance in vivo.* European journal of nuclear medicine, 1999. **26**(3): p. 283-293.

[19] Ponto, J.A., *Mechanisms of radiopharmaceutical localization.* UNM College of Pharmacy, 2012. **16**(4).

[20] Vallabhajosula, S. and A. Owunwanne, *Pathophysiology and mechanisms of radiopharmaceutical localization*, in *The pathophysiologic basis of nuclear medicine*. 2006, Springer. p. 29-49.

[21] Tsopelas, C., *Radiotracers used for the scintigraphic detection of infection and inflammation.* The Scientific World Journal, 2015. **2015**.

[22] Miot-Noirault, E., et al., *Scintigraphic in vivo assessment of the development of pulmonary intravascular macrophages in liver disease: experimental study in rats with biliary cirrhosis.* Chest, 2001. **120**(3): p. 941-947.

[23] Schindl, M.J., et al., *The adaptive response of the reticuloendothelial system to major liver resection in humans.* Annals of surgery, 2006. **243**(4): p. 507.

[24] Saha, G.B., et al., *Experience with technetium-99m albumin colloid kit for reticuloendothelial system imaging.* Journal of nuclear medicine technology, 1986. **14**(3): p. 149-151.

[25] Hunt, A., et al., *Preparation of Tc-99m-macroaggregated albumin from recombinant human albumin for lung perfusion imaging.* European journal of pharmaceutics and biopharmaceutics, 2006. **62**(1): p. 26-31.

[26] Gandhi, S.J., et al., *Tc-99m macro aggregated albumin scintigraphy - indications other than pulmonary embolism: A pictorial essay.* Indian journal of nuclear medicine : IJNM : the official journal of the Society of Nuclear Medicine, India, 2013. **28**(3): p. 152-162.

[27] Levine, G., *Tc-99m MAA: A Model for Administering the Desired Number of Particles for Pulmonary Perfusion Studies.* Journal of Nuclear Medicine Technology, 1980. **8**(1): p. 33-36.

[28] Gandhi, S.J., et al., *Tc-99m macro aggregated albumin scintigraphy–Indications other than pulmonary embolism: A pictorial essay.* Indian Journal of Nuclear Medicine: IJNM: The Official Journal of the Society of Nuclear Medicine, India, 2013. **28**(3): p. 152.

[29] Som, P., et al., *Detection of gastrointestinal blood loss with 99mTc-labeled, heat-treated red blood cells.* Radiology, 1981. **138**(1): p. 207-209.

[30] Ehrlich, C.P., et al., *Splenic scintigraphy using Tc-99m-labeled heat-denatured red blood cells in pediatric patients: concise communication.* Journal of nuclear medicine: official publication, Society of Nuclear Medicine, 1982. **23**(3): p. 209-213.

[31] Khandan, A., E. Karamian, and M. Bonakdarchian, *Mechanochemical synthesis evaluation of nanocrystalline bone-derived bioceramic powder using for bone tissue engineering.* Dental Hypotheses, 2014. **5**(4): p. 155.

[32] Czernin, J., N. Satyamurthy, and C. Schiepers, *Molecular mechanisms of bone 18F-NaF deposition.* Journal of Nuclear Medicine, 2010. **51**(12): p. 1826-1829.

[33] Silberstein, E.B. *Systemic radiopharmaceutical therapy of painful osteoblastic metastases*. in *Seminars in radiation oncology*. 2000. Elsevier.

[34] Bokhari, S., et al., *99mTc-pyrophosphate scintigraphy for differentiating light-chain cardiac amyloidosis from the transthyretin-related familial and senile cardiac amyloidoses.* Circulation: Cardiovascular Imaging, 2013. **6**(2): p. 195-201.

[35] Russell, R.G.G., *Bisphosphonates: mode of action and pharmacology.* Pediatrics, 2007. **119**(Supplement 2): p. S150-S162.

[36] Dewanjee, M.K. and P.C. Kahn, *Mechanism of localization of*

99mTc-labeled pyrophosphate and tetracycline in infarcted myocardium. J Nucl Med, 1976. **17**(7): p. 639-46.

[37] Mulligan, J.S., P.W. Blue, and J.A. Hasbargen, *Methods for measuring GFR with technetium-99m-DTPA: an analysis of several common methods.* J Nucl Med, 1990. **31**(7): p. 1211-9.

[38] Taylor, A.T., *Radionuclides in nephrourology, part 1: radiopharmaceuticals, quality control, and quantitative indices.* Journal of Nuclear Medicine, 2014. **55**(4): p. 608-615.

[39] Elgazzar, A.H., *Basis of Radiopharmaceutical Localization*, in *Synopsis of Pathophysiology in Nuclear Medicine*. 2014, Springer. p. 27-40.

[40] Palestro, C.J., *Radionuclide Imaging of Musculoskeletal Infection: A Review.* J Nucl Med, 2016. **57**(9): p. 1406-12.

[41] Signore, A., et al., *Clinical indications, image acquisition and data interpretation for white blood cells and anti-granulocyte monoclonal antibody scintigraphy: an EANM procedural guideline.* Eur J Nucl Med Mol Imaging, 2018. **45**(10): p. 1816-1831.

[42] McAfee, J.G. and M.L. Thakur, *Survey of radioactive agents for in vitro labeling of phagocytic leukocytes. I. Soluble agents.* J Nucl Med, 1976. **17**(6): p. 480-7.

[43] Ordonez, A.A. and S.K. Jain, *Pathogen-Specific Bacterial Imaging in Nuclear Medicine.* Semin Nucl Med, 2018. **48**(2): p. 182-194.

[44] Salmanoglu, E., S. Kim, and M.L. Thakur, *Currently Available Radiopharmaceuticals for Imaging Infection and the Holy Grail.* Semin Nucl Med, 2018. **48**(2): p. 86-99.

[45] Elgazzar, A.H., *Synopsis of pathophysiology in nuclear medicine.* 2014.

[46] Strauss, H.W., *Nuclear oncology : pathophysiology and clinical applications.* 2013.

[47] Li, Z.-B., et al., *The Synthesis of 18F-FDS and Its Potential Application in Molecular Imaging.* Molecular Imaging and Biology, 2008. **10**(2): p. 92-98.

[48] Zhu, W., et al., *Biodistribution and Radiation Dosimetry of the Enterobacteriaceae-Specific Imaging Probe [18F]Fluorodeoxysorbitol Determined by PET/CT in Healthy Human Volunteers.* Molecular Imaging and Biology, 2016. **18**(5): p. 782-787.

[49] Welling, M.M., et al., *An update on radiotracer development for molecular imaging of bacterial infections.* Clinical and Translational Imaging, 2019. **7**(2): p. 105-124.

[50] Palestro, C.J., *The current role of gallium imaging in infection.* Seminars in Nuclear Medicine, 1994. **24**(2): p. 128-141.

[51] Wester, H.J., et al., *Synthesis and radiopharmacology of O-(2-[18F] fluoroethyl)-L-tyrosine for tumor imaging.* J Nucl Med, 1999. **40**(1): p. 205-12.

[52] Sharma, R., et al., *A comparison study of (11)C-methionine and (18) F-fluorodeoxyglucose positron emission tomography-computed tomography scans in evaluation of patients with recurrent brain tumors.* Indian journal of nuclear medicine : IJNM : the official journal of the Society of Nuclear Medicine, India, 2016. **31**(2): p. 93-102.

[53] Hodolic, M., *Role of (18)F-choline PET/CT in evaluation of patients with prostate carcinoma.* Radiology and oncology, 2011. **45**(1): p. 17-21.

[54] Welle, C.L., et al., *11C-Choline PET/CT in Recurrent Prostate Cancer and Nonprostatic Neoplastic Processes.* RadioGraphics, 2016. **36**(1): p. 279-292.

[55] Cornell, R. and N. Ridgway, *CTP: phosphocholine cytidylyltransferase: Function, Regulation, and Structure of an amphitropic enzyme required for membrane biogenesis.* Progress in lipid research, 2015. **59**.

[56] Spick, C., K. Herrmann, and J. Czernin, *Evaluation of prostate cancer with 11C-Acetate PET/CT.* Journal of Nuclear Medicine, 2016. **57**: p. 30S–37S.

[57] Smith, G., et al., *Synthesis and evaluation of nucleoside radiotracers for imaging proliferation.* Nucl Med Biol, 2012. **39**(5): p. 652-65.

[58] Zhang, Z., et al., *Positron Emission Tomography Imaging with 2-[(18) F]F- p-Aminobenzoic Acid Detects Staphylococcus aureus Infections and Monitors Drug Response.* ACS Infect Dis, 2018. **4**(11): p. 1635-1644.

[59] Xu, Z., et al., *(18) F-Fluoromisonidazole in tumor hypoxia imaging.* Oncotarget, 2017. **8**(55): p. 94969-94979.

[60] Bae, Y.H. and K. Park, *Targeted drug delivery to tumors: myths, reality and possibility.* Journal of controlled release, 2011. **153**(3): p. 198.

[61] Livingston, R.B., et al., *In vitro determination of thymidine-3H labeling index in human solid tumors.* Cancer research, 1974. **34**(6): p. 1376-1380.

[62] Abdalla, A.M.E., et al., *Engineered nanoparticles: thrombotic events in cancer.* Nanoscale, 2014. **6**(23): p. 14141-14152.

[63] Winchell, H.S. *Mechanisms for localization of radiopharmaceuticals in neoplasms*. Elsevier.

[64] Wells, P., et al., *Assessment of proliferation in vivo using 2-[11C] thymidine positron emission tomography in advanced intra-abdominal malignancies.* Cancer research, 2002. **62**(20): p. 5698-5702.

[65] Shields, A.F., *PET imaging of tumor growth: not as easy as it looks.* Clinical cancer research, 2012. **18**(5): p. 1189-1191.

[66] Chen, X. and S. Wong, *Cancer theranostics*. 2014: Academic Press.

[67] Moreau, A., et al., *Contribution of Different Positron Emission Tomography Tracers in Glioma Management: Focus on Glioblastoma.* Frontiers in Oncology, 2019. **9**.

[68] Sun, H., et al., *Imaging DNA synthesis with [18 F] FMAU and positron emission tomography in patients with cancer.* European journal of nuclear medicine and molecular imaging, 2005. **32**(1): p. 15-22.

[69] Patel, Y.C., et al., *The somatostatin receptor family.* Life sciences, 1995. **57**(13): p. 1249-1265.

[70] Fani, M., P.K. Peitl, and I. Velikyan, *Current status of radiopharmaceuticals for the theranostics of neuroendocrine neoplasms.* Pharmaceuticals, 2017. **10**(1): p. 30.

[71] Virgolini, I., et al., *Somatostatin receptor subtype specificity and in vivo binding of a novel tumor tracer, 99mTc-P829.* Cancer Research, 1998. **58**(9): p. 1850-1859.

[72] Virgolini, I., et al., *Cross-competition between vasoactive intestinal peptide and somatostatin for binding to tumor cell membrane receptors.* Cancer research, 1994. **54**(3): p. 690-700.

[73] Horti, A.G., et al., *18F-ASEM, a radiolabeled antagonist for imaging the α7-nicotinic acetylcholine receptor with PET.* Journal of Nuclear Medicine, 2014. **55**(4): p. 672-677.

[74] Pérez-Medina, C., et al., *PET imaging of tumor-associated macrophages with 89Zr-labeled high-density lipoprotein nanoparticles.* Journal of Nuclear Medicine, 2015. **56**(8): p. 1272-1277.